Iowa State University
Digital Repository

1970

The radioactive decay of 190Re and isomer ratio measurements in photonuclear reactions

Peter Eugene Haustein

Iowa State University

Follow this and additional works at: https://lib.dr.iastate.edu/rtd

Part of the Nuclear Commons, Physical Chemistry Commons, and the Radiochemistry Commons

Recommended Citation

70-25,790

HAUSTEIN, Peter Eugene, 1944-

THE RADIOACTIVE DECAY OF ^{190}Re AND ISOMER
RATIO MEASUREMENTS IN PHOTONUCLEAR REACTIONS.

Iowa State University, Ph.D., 1970
Chemistry, physical

University Microfilms, A XEROX Company , Ann Arbor, Michigan

THE RADIOACTIVE DECAY OF ^{190}Re AND ISOMER RATIO

MEASUREMENTS IN PHOTONUCLEAR REACTIONS

by

Peter Eugene Haustein

A Dissertation Submitted to the

Graduate Faculty in Partial Fulfillment of

The Requirements for the Degree of

DOCTOR OF PHILOSOPHY

Major Subject: Physical Chemistry

Approved:

In Charge of Major Work

Head of Major Department

Dean of Graduate College

Iowa State University
Ames, Iowa

1970

TABLE OF CONTENTS

PREFACE

Studies of nuclear structure fall into two areas: on the one hand those properties deduced from the spontaneous decay of radioisotopes, and on the other hand, those properties deduced from measurements of nuclear reaction processes. Both of these areas continue to be active fields of research providing new information, often in a complementary manner, concerning the static and dynamic properties of the ever increasing number of nuclei that can be produced and studied by the experimentalist. The thesis which follows summarizes experimental work done in both of these areas.

PART I. THE RADIOACTIVE DECAY OF ^{190}Re

I. INTRODUCTION

A. Historical Aspects

Since the discovery of natural radioactivity by Becquerel (1) in 1896 and the production of the first synthetic radioisotopes in 1934 (2), a large number of studies have been undertaken in an attempt to classify the various disintegration modes of the decaying nucleus and to measure the intensity and energies of the various particles produced or ejected by a radioactive nucleus and its surrounding atomic electrons. The concurrent development of radiation detection apparatus has provided powerful spectroscopic tools for these studies of nuclear transformations and their associated radiations. The first attempts to correlate these observations with theoretical descriptions of the nucleus had little success. It was not until the development of the beta decay theory in the 1930's (3) and the origination of the nuclear shell model in the late 1940's (4, 5) that successful correlation of observed nuclear properties with a theoretical understanding of the nuclear structure was possible.

B. Purpose of the Investigation

This portion of the thesis describes the investigation of the nuclear decay scheme of ^{190}Re and indicates the relevance of its decay properties to the current strong theoretical interest in nuclei with A ~ 190. The original

suggestion for the study of the ^{190}Re decay was that of Dr. D. Reuland[1] who pointed out that daughter radiations from ^{190}Re as produced by the beta decay of ^{190}W as the parent could be used as evidence for the production of ^{190}W, a previously unreported isotope, which it was hoped could be synthesized by the reaction ^{192}Os(γ,2p)^{190}W. A check of the available literature concerning the ^{190}Re decay, described below in greater detail, revealed that ground and isomeric states had been produced and assigned to ^{190}Re and that some characteristic gamma rays following the decay of these levels had been observed. However several features seemed ambiguous. Although the ^{190}Re decay seemed consistent with independently determined features of the ^{190}Os energy levels into which it decayed, several additional unreported gamma-ray transitions must accompany the ^{190}Re decay based on analogous transitions in the ^{190}Ir → ^{190}Os decay which populated similar levels in ^{190}Os. It was felt that a reinvestigation of the ^{190}Re decay scheme employing high resolution Ge(Li) gamma-ray detectors could be used to clarify the decay of this nuclear species and provide new information about ^{190}Os into which it decays.

C. Literature Survey

The first report of the production of the double odd nucleus ^{190}Re was that of Aten and de Feyfer (6). A

---

[1]D. Reuland, Indiana State University. Private communication. 1967.

2.8 ± 0.5 min activity resulting from either fast neutron or 26 MeV deuteron irradiation of osmium was assigned to the decay of the ground state of ^{190}Re. This activity was observed to decay by β^- emission with an energy of 1.8 MeV as determined by absorption measurements. The activity also had gamma rays of 191, 392, 569, and 830 keV associated with its decay. On the basis of similar energy gamma-ray transitions observed in the ^{190}Ir $\rightarrow$ ^{190}Os decay, it appeared that the activity decayed strongly to the 1387 keV level of ^{190}Os, thereby establishing its assignment to ^{190}Re. Log $\underline{ft}$ calculations indicated that ^{190}Re would have a ground state spin and parity of $\leq 4^-$. Baro and Flegenheimer (7) reported what was thought to be an isomeric state of ^{190}Re decaying with a half-life of 2.8 hrs, which was isolated in the chemically separated rhenium fraction of either iridium irradiated with fast neutrons or ^{192}Os with 28 MeV deuterons. This activity was reported to decay with a 1.6 - 1.7 MeV beta ray followed by gamma rays of 122, 210, 375, 560, and 820 keV. No decay scheme was suggested. An attempt to separate the 2.8 minute activity from the 2.8 hour isomer via a Szilard-Chalmers process was made. The negative result was taken as an indication that the two states decayed independently by β^- emission and that if an isomeric transition occurred between the two states, it was not highly internally converted.

Much additional information about the ^{190}Os levels has

been published in connection with studies of the ground and double isomeric state radioactivity of ^{190}Ir (8), from neutron capture gamma-ray spectroscopy of the reaction ^{189}Os(n,γ)^{190}Os (9) and from charged particle excitation of the ^{190}Os nucleus (10). A fairly complete picture of the ^{190}Os levels and transitions has emerged which indicated that the ^{190}Re decay should be more complicated than that so far reported.

II. TECHNIQUES FOR DECAY SCHEME STUDIES

Techniques for the study of nuclear decay schemes involve three different kinds of tasks which are described below in connection with the investigation of the ^{190}Re decay properties. These areas are: 1) A suitable production method for the desired activity must be chosen. Following the actual production of the isotope, sample preparation (chemical, physical, or both) must be performed prior to counting. 2) Various radiation detectors are employed to measure and analyze the radiation emitted from the source. Such counting procedures typically utilize detectors selectively sensitive to the various decay modes of the nucleus under study. Detectors are used to measure the energies and intensities of particles emitted in the decay and to follow the decay process in time to measure the characteristic half-life of the radioactive nucleus being studied. In addition sequential decay processes can be observed by using more than one detector at a time; such observations being used to verify the order in which decay events occur. 3) The data accumulated in the counting experiments must be interpreted and formulated into a decay scheme consistent with the observations and the physical process of radioactive decay. This typically concerns the chemical and mass number assignment to the activity based on the decay mode of nuclide produced. In addition the energy, intensity,

and half-life measurements are used to construct the
pattern by which the radioactive nucleus de-excites, and
they provide indications of the nuclear structure of the
parent and daughter nuclides involved in the decay process.
Once this decay scheme has been established, theoretical
models and calculations may be applied for understanding
the nuclear structure and properties of the isotopes in
question.

The following is a discussion of the application of
these three procedures to the ^{190}Re decay. It is not meant
to be a detailed presentation of the work done on the ^{190}Re
decay (Sections III, IV, and V of this portion of the thesis
contains such material) but rather as an overview of the
topic for reader's benefit in understanding the methods
used in the ^{190}Re investigation.

The method chosen for the production of the ^{190}Re
sources was high energy photon irradiation of small amounts
of ^{192}Os metallic powder. Gamma rays with a maximum energy
of 70 MeV were produced in the ISU synchrotron and used to
bombard the ^{192}Os targets. Five radioactive products were
observed, the ground and isomeric states of ^{191}Os, ^{191}Re,
^{190m}Os, and ^{190}Re, the desired product. These products
represent the results of the reactions (γ,n), (γ,p), $(\gamma,2n)$,
and (γ,np) respectively. Despite the presence of the four
additional side products, their half-lives and decay

properties allowed all counting experiments to be successfully performed without chemical treatment or destruction of the ^{192}Os target material.

Sources, thus prepared, were counted using a variety of equipment described more fully in Section III of this portion of the thesis. A high resolution Ge(Li) gamma-ray detector was used to accumulate the gamma ray spectra from the source. Beta spectra were accumulated using an organic scintillation crystal. Additional detectors were used in conjunction with a single channel pulse height analyzer to evaluate the half-lives of the various radioactive products in the source. Gamma-gamma coincidence counting was employed to confirm the gamma ray cascade pattern in the energy level scheme of ^{190}Os to which ^{190}Re decays. Computer analysis of the data as described in Section III provided fast, accurate and efficient data reduction.

Construction of the ^{190}Re decay scheme was greatly aided by the substantial experimental information already gathered about ^{190}Os. In addition confirmation experiments utilizing the ^{190}Ir → ^{190}Os decay proved helpful in clarifying the ^{190}Re → ^{190}Os decay. A self consistent decay scheme was developed, parts of which were independently confirmed later by other experimenters.

III. EXPERIMENTAL

A. Target Materials

Sources of ^{190}Re were prepared by synchrotron irradiation of small amounts of isotopically enriched ^{192}Os metallic powder. Two hundred milligrams of ^{192}Os enriched to > 98 percent in ^{192}Os were obtained from the Stable Isotopes Division of the U.S.A.E.C. Oak Ridge National Laboratory. Table 1 shows the sample composition as reported by the suppliers. No additional purification was performed on the target materials. The powder was dried at 110° C prior to irradiation to reduce ^{15}O activity induced in the sample from moisture in the target material.

B. Irradiation Procedure

Samples of approximately 75 mg ^{192}Os metal powder were placed in previously dried small aluminum irradiation cans in the form of right circular cylinders approximately 5 mm in diameter and 8 mm high. The filled irradiation can was then mounted into a spring loaded aluminum holding bracket on the end of a plastic Synthane probe which was inserted into the interior of the donut of the Iowa State synchrotron, and rotated until the can was positioned to intercept the beam along its length. The probe stick was fastened to prevent movement of the can during the irradiation.

All samples were irradiated as described above at the

Table 1. Isotopic analysis of the ^{192}Os target material

Osmium isotope	Atomic percent	Precision
184	< 0.05	-
186	< 0.05	-
187	< 0.05	-
188	0.19	$\pm$ 0.05
189	0.30	0.05
190	0.78	0.05
192	98.7	0.1

internal probe position of the synchrotron. Bremsstrahlung was produced by the collision of 70 MeV electrons accelerated in the synchrotron donut with a target consisting of a lead plate approximately 2.8 mm thick located in front of the sample. A description of the synchrotron and its associated equipment has been reported elsewhere (11,12,13). Irradiation times varied from 5 to 15 min depending on the intensity and stability of the beam. A 13.5 hr irradiation was performed on ~ 75 mg of natural isotopic distribution powdered iridium metal used in confirmation experiments described later. In attempts to produce the 2.8 hr ^{190}Re isomer, irradiations of up to 2 hours duration were used on the ^{192}Os targets.

C. Sample Transfer and Preparation

At the conclusion of the irradiation period, the target can was removed from the probe assembly, placed into a polyethylene transfer rabbit, and inserted into the pneumatic tube for transfer to the counting laboratory at the reactor building. A timing device located at the reactor building counting room was programmed to start a set of timers to indicate elapsed time after the end of the irradiation. On arrival at the reactor building the sample was removed from the irradiation can and placed into a plastic test tube and, if gamma-ray counting was to be employed, positioned for counting. Typically these operations were performed in about two minutes. In the case of beta-ray counting, the target was spread over an area of about 3 cm^2 on a thin plastic disk to reduce effects of attenuation of the beta spectrum.

D. Counting Equipment

For the accumulations of singles gamma-ray spectra the counting equipment consisted of a 20 cc Ge(Li) detector (Nuclear Diodes Model LGC 3.5X) and its associated electronics (TMC Model TC 135 preamp, Canberra Industries Model 1416 amplifier). The detector was operated at 1650 volts bias and had a resolution (full-width at half maximum) of 4.5 keV for the 661.6 keV ^{137}Cs line. Data were stored in a 1600 channel pulse height analyzer (RIDL Model 24-3) which

had punched paper tape and printed listing output devices.

Beta-ray spectra were accumulated by using a 3.8 x 2.2 cm stilbene beta phosphor obtained from Crystals Inc. coupled to a photomultiplier tube operated at 935 volts bias. Pulses from the phototube were routed into the internal amplifiers of 1600 channel analyzer and stored in a 400 channel sub-group of the analyzer's memory.

A single channel analyzer with a paper tape output lister was used in conjunction with the beta phosphor described above or with a 3 inch solid NaI(Tl) crystal to multiscale various energy ranges of either the beta or gamma activity of the source. Sequential count accumulations of this type were used to construct decay curves and for evaluations of half-lives.

Gamma-gamma two parameter coincidence spectra were accumulated for use in verifying the proposed ^{190}Re decay scheme. A 7.8 x 7.8 cm solid NaI(Tl) crystal was mounted 90° relative to the Ge(Li) diode, and positioned so that the ^{190}Re source would be approximately 2.5 cm from the face of either detector. The dual analog-to-digital converters of the analyzer were employed to store data in a 40 x 40 channel coincidence array, using separate energy gains for the two detector systems.

E. Data Preparation Procedure

Virtually all the data accumulated by the above proce-
dures were, in part, analyzed using one or more FORTRAN-IV
computer programs. This necessitated the conversion of the
data either in punched paper tape form or printed listings
to standard 80 columns IBM computer input cards. Data in
the form of printed listing were punched onto cards by hand.
Data in the form of punched paper tape were either converted
to cards using the IBM 047 Tape-to-Card-Printing-Punch
located at the synchrotron building or were recorded on
IBM 7-track magnetic tape, using a facility at the Cyclone
computer lab. The magnetic tapes were then directly process-
ible on the IBM 360/65 computer at the Computation Center.

F. Computer Programs

The following are short descriptions of the computer
programs used in the data analysis.

ICPEAX-, a program originally written by P. J. M.
Korthoven and modified by the author, was used for auto-
matic photopeak detection in γ-ray spectra accumulated using
the Ge(Li) diode. The program also fit Gaussians to the
photopeaks, determining channel locations, peak widths and
areas. Energy calibration features of the program permitted
calculation of the photopeak energies. A plotting routine
incorporated in the program produced semi-log plots of the

spectra.

SMASH-, this program also written by P. J. M. Korthoven (14), was used in the analysis of the decay curves measured for the ^{190}Re sources. The program was used to evaluate the half-lives of the radioactive components in the source, from both the beta and gamma multiscaled data obtained from the single channel analyzer.

KURIE-, a program written by the author, was used to perform calculations for the conventional Kurie plot analysis of beta-ray spectra. The data obtained from beta singles spectra accumulated using the stilbene beta phosphor were analyzed by KURIE and plots of either the raw beta spectrum or the Kurie analysis could be obtained from the program for later use in visual resolution of the beta components.

BONNIE-, a program written by the author, was designed to perform the calculations for measurements of the Ge(Li) detector photopeak detection efficiency. Counting data from a series of calibrated gamma-ray sources were used as input to the program. The detector efficiency as a function of energy was calculated and a polynomial function in the energy was fit to the data points. Once this function was determined, the program could be instructed to make detection efficiency corrections to photopeak areas and to normalize the gamma-ray intensities from the ^{190}Re source.

IV. EXPERIMENTAL RESULTS AND DISCUSSION

A. Isotopic Assignment,
Gamma-Ray Spectra and Energies

It was decided that the best way to identify the presence of ^{190}Re in targets of synchrotron irradiated ^{192}Os was by the use of gamma-ray spectroscopy. Spectra would be accumulated shortly after the end of the irradiation in an attempt to observe the gamma rays assigned to the ^{190}Re activity by Aten (6). Accordingly synchrotron irradiations of 2-5 minutes duration were performed so that the yield of ^{190}Re would be maximized in relation to the other likely products of the irradiation: 10 min ^{191}Re, 10 min ^{190m}Os, 14 hr ^{191m}Os, 15 day ^{191}Os. The choice of 2-5 minutes irradiation was based on the 2.8 $\pm$ 0.5 min half-life for ^{190}Re observed by Aten (6). At the end of the irradiation, the target container was transported to the reactor building using the pneumatic tube between the synchrotron and reactor. Initially, NaI(Tl) detectors were used to accumulate the gamma ray spectrum of the source. Positive evidence for the presence of ^{190}Re in the source could not be obtained using these detectors, despite the short delay of approximately 2 minutes before counting started which minimized the loss of ^{190}Re by its decay. The poor resolution of the NaI(Tl) detectors coupled with the rather strong interference due to prominent gamma rays of ^{190m}Os prevented unambiguous identi-

fication of gamma rays from ^{190}Re. Therefore, a Ge(Li)
detector was employed to take advantage of its higher
resolution. Although this type of detector is inherently
less efficient for gamma ray detection, its much greater
resolving power allowed observation of the ^{190}Re gamma-ray
lines in the spectrum despite the unavoidable presence of
the ^{190m}Os interference. A typical spectrum accumulated
approximately 2 minutes after the irradiation using the
Ge(Li) detector is shown in Figure 1. The transitions at
187, 397-407, 556-569 and 829-839 keV agree closely with
those reported by Aten (6). Moreover they are identical to
transitions observed to depopulate ^{190}Os levels reached by
other processes (8). The only irradiation product from
^{192}Os targets that could populate these ^{190}Os levels would
be ^{190}Re and its associated beta-minus decay. In Figure 2
the gamma-ray spectrum of the source ~ 20 minutes after the
irradiation is shown. The disappearance of the lines at
199, 224, 371, 397, 407, 431, 557, 569, 605, 631, 768, 829,
839, 1200, and 1387 keV indicated the presence of an activity
shorter lived than 10 min. ^{190m}Os which has gamma rays at
187, 361, 502, and 615 keV (15), and again suggested the 2.8
min activity seen by Aten. The transition at 129 keV was
assigned to 15 day ^{191}Os based on its energy and long life
(16). This 129 keV line was also observed to grow in
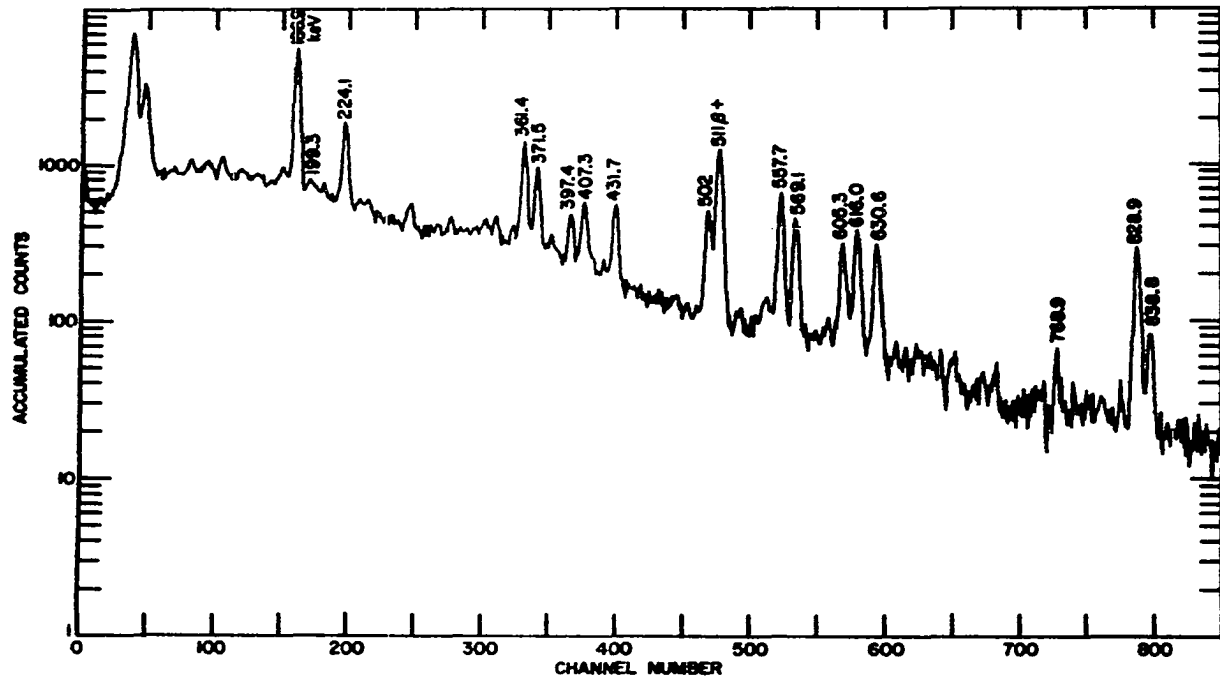intensity following the irradiation, and then to decay.

Figure 1.   Gamma-ray spectrum of the ^{190}Re source two minutes after the irradiation

17
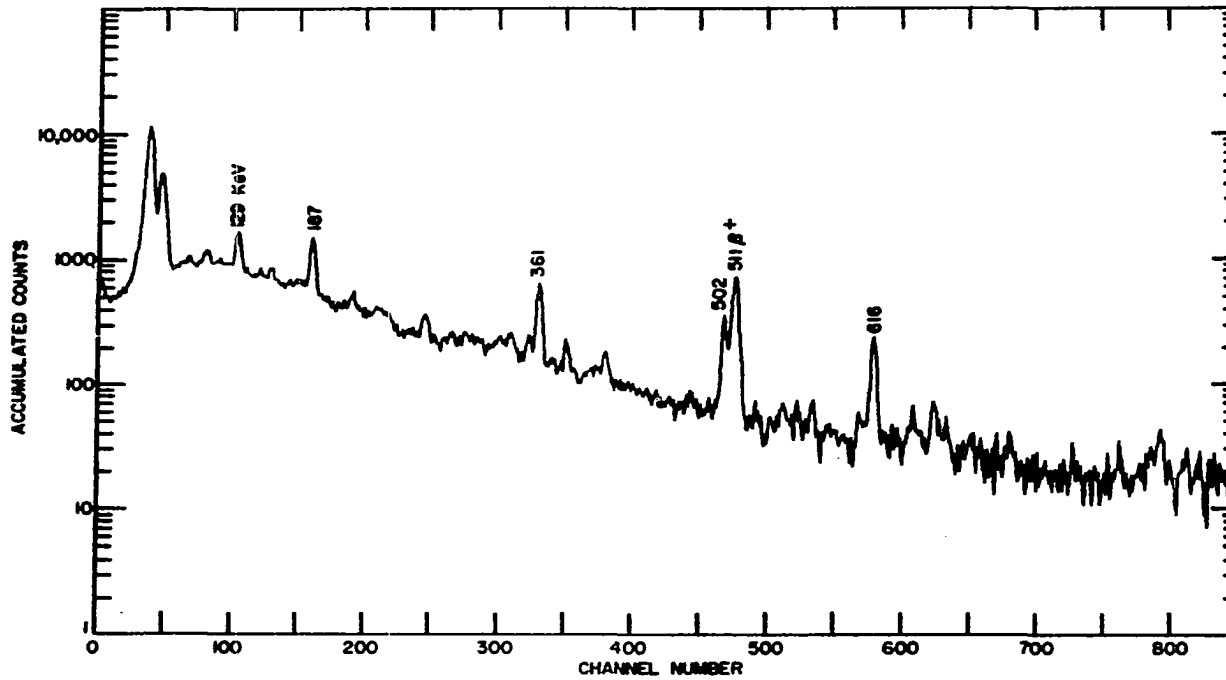
Figure 2.   Gamma-ray spectrum of the ^{190}Re source 20 minutes after the irradiation

This was used to infer the presence of 14 hour ^{191m}Os in

the source. Its decay to ^{191}Os, by a 14 keV isomeric

transition which was unobservable due to the strong x-ray

lines of slightly higher energy, would account for the

growth and decay properties of the 129 keV transition. On

the basis of beta-ray measurements described below, the

presence of 10 min ^{191}Re in the source was also inferred.

In Table 2 the various radioactive reaction products pro-

duced by synchrotron irradiation of ^{192}Os are listed, along

with their half-lives and production reactions.

Table 2. Radioactive products from synchrotron irradiation
of ^{192}Os

Product nucleus	Half-life	Reaction
^{190}Re	3.1 ± 0.3 min	^{192}Os(γ,np)
^{190m}Os	9.9 min	^{192}Os(γ,2n)
^{191}Os	15.0 day	^{192}Os(γ,n)
^{191m}Os	14.0 hour	^{192}Os(γ,n)
^{191}Re	9.7 min	^{192}Os(γ,p)

In addition to those gamma rays which decayed out in

the interval between the data of Figures 1 and 2, the

transitions at 187 and 361 keV are also part of the ^{190}Re

decay as well as being part of the ^{190m}Os decay. This point

is more fully discussed in later parts of this section. In Table 3 the energies of the gamma rays for ^{190}Re are listed. These energies are based on the calibration of the 1600 channel analyzer using a set of gamma-ray standards obtained from the International Atomic Energy Agency. The gamma-ray energies of the standards are based on a recent compilation (17). The ICPEAX program was used to provide linear and quadratic fits of the calibration points based on the photopeak locations in the spectrum of the standards, and the location of gamma rays in the spectra of the source.

B. Half-life Measurements

Following the identification of the gamma-ray lines due to ^{190}Re, its half-life was determined by time-sequenced multi-scaling of the ^{190}Re gamma and beta radiation. Since the gamma rays above 615 keV are due solely to ^{190}Re observation of the decay of the gamma radiations above that energy would yield the ^{190}Re half-life. Sources of ^{190}Re were counted with a NaI(Tl) detector coupled to a single channel analyzer that was set to count only events with energies > 750 keV. Counts accumulated in each time interval were printed on the paper tape printing lister coupled to the single channel analyzer. Two such measurements were made over a time span of several ^{190}Re half-lives until the counting rates were primarily due to background radiation. In Figure 3 one of decay curves is shown. Computer analysis of the decay

Table 3.   Gamma ray energies for the ^{190}Re decay

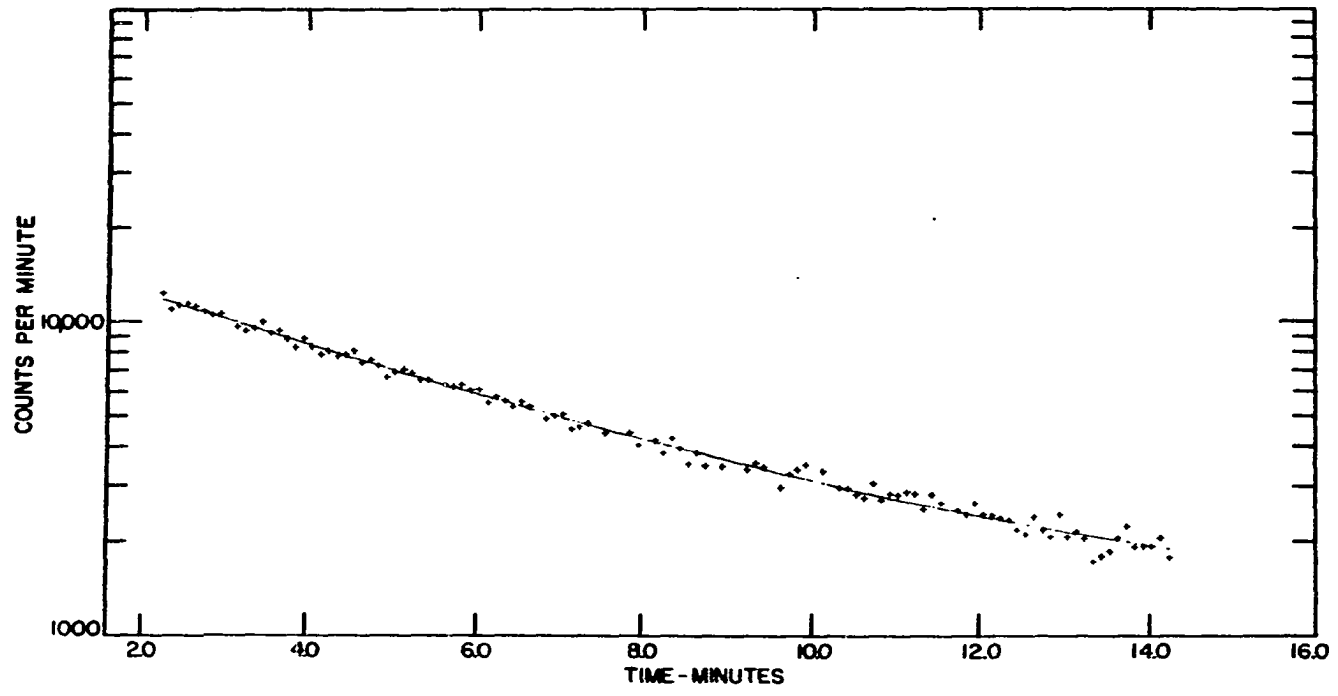| Energies	Uncertainty in the energies
186.9 keV $\pm$	0.1 keV
199.3	1.4
224.1	0.1
361.4	0.1
371.5	0.1
397.4	0.3
407.3	0.3
431.7	0.2
557.7	0.2
569.1	0.2
605.3	0.3
630.6	0.3
768.9	0.5
828.9	0.2
838.8	0.4
1200.3	0.6
1387.7	1.5

Figure 3. Decay curve of the [190]Re gamma-ray activity

curves was made using SMASH (14). Two component fits were used to resolve the decay curve into the ^{190}Re portion and a time-independent portion representing the background. For both measurements the program was allowed to vary the initially estimated 2.8 min half-life until the best fit to the data was obtained. The portion of the activity assigned to the background agreed closely with the background counting rates observed with the source removed. Experience with the program indicated that better fits are obtained if the program is allowed to fit the background portion of the data, rather than specifying the background counting rate to be used to correct the decay curve prior to computer resolution. The agreement between the computer resolved background activity and the observed count rate due to the background indicated that no serious errors are introduced by this method. The computer assigned half-lives for the ^{190}Re activity were 3.18 and 3.25 minutes in the two measurements.

In addition a measurement of the ^{190}Re half-life was made by multiscaling the beta radiation of the source. The beta phosphor described in Section III was coupled to the single channel analyzer and lister. This system was set to count beta events with energies > 150 keV. A decay curve of the beta activity was measured in the same way as for the gamma-ray cases, and is shown in Figure 4. Computer analysis of the decay curve was again made, using a three component
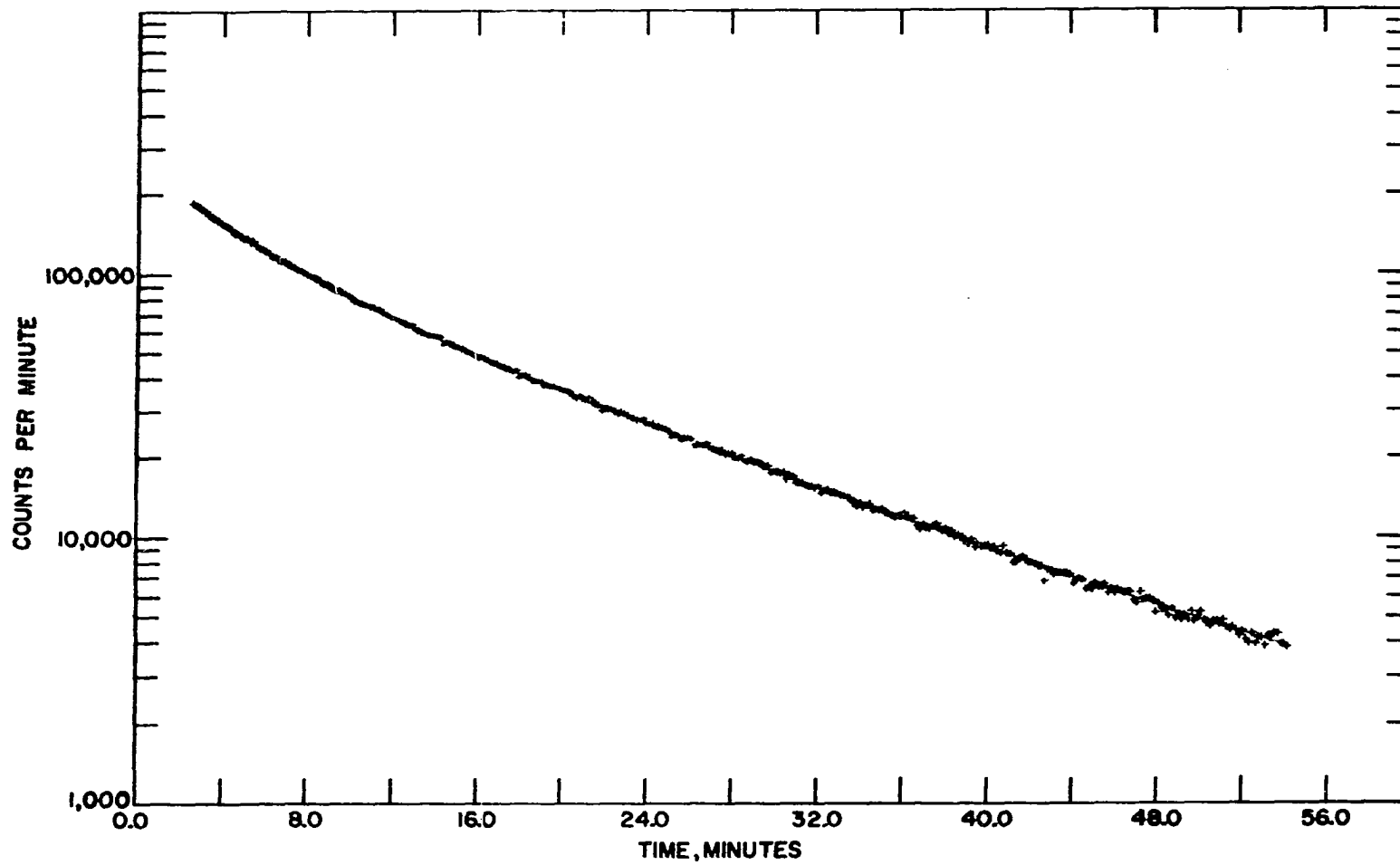
Figure 4.   Decay curve of the ^{190}Re beta-ray activity

fit instead of the two components in the gamma ray decay curves. The three component fit was used for two reasons. Internal conversion of the 10 min ^{190m}Os gamma rays would yield electrons with energies > 150 keV and would therefore contribute to the decay curve. The previously reported pure beta emitting ^{191}Re activity (18) would be present in the source and would also contribute to the decay curve. The moderate yield of the ^{190}Re produced by ^{192}Os(γ,np) indicated that ^{191}Re, produced by ^{192}Os(γ,p), would be of at least comparable yield, and probably of much higher yield owing to the general trend of decreasing reaction cross section as more nucleons are ejected in photonuclear activation. Results of the computer fit are shown in Table 4.

Table 4. Results of the computer resolved beta decay curve

Nuclide	Half-life found	Count rate at the end of the irradiation (counts/minute)
^{190}Re	2.90 min	119,795
^{190m}Os, ^{191}Re	9.70	142,412
Background radiation	-	928

The yield of the 9.7 min activity is a sum of contributions due to ^{190m}Os conversion electrons and ^{191}Re beta particles, the latter contribution being greater based on the small internal conversion coefficients for the ^{190m}Os gamma rays (15). The similarity of half-lives for these two isotopes prevented any better resolution of these decay curves.

The average and deviation of the three half-life determinations is 3.11 $\pm$ 0.20 min. This value was used in all subsequent decay corrections for ^{190}Re and in log $\underline{ft}$ calculations described later.

C. Gamma-Ray Transition Intensities

Gamma-ray transition intensities from a pure radio-active source are usually reported in terms of a relative scale, with one transition assigned an arbitrary intensity and the other transition intensities adjusted to this scale. This is the most convenient method for interpretation of beta-ray feeding of excited states of daughter nucleus. In the case of ^{190}Re, sources were counted at a position above the Ge(Li) detector for which the detector efficiency had been previously measured. The photopeak areas for the ^{190}Re gamma rays were then corrected for the detector's varying efficiency with energy and one of the ^{190}Re lines, the 224 keV transition, was assigned an intensity of 100. The other transition intensities were calculated relative to

the 224 keV line by dividing the efficiency corrected photo-peak intensity of the transition by the corresponding corrected intensity of the 224 keV line and multiplying by 100.

The detector efficiency was measured for sources counted 10.0 cm directly above the detector face and on the cyclindrical axis of the Ge(Li) crystal housing. Standard sources of ^{57}Co, ^{22}Na, ^{137}Cs, ^{54}Mn, ^{88}Y, and ^{60}Co prepared by the International Atomic Energy Agency were counted at this geometry for 30 live time minutes each. These sources had been calibrated for the yield of gamma rays per disintegration and for the absolute disintegration rate on January 1, 1968 by the I.A.E.A. Gamma-ray spectra of the standard sources were computer analyzed by the ICPEAX program to obtain the photopeak intensities. The detector efficiency at the energy of the particular standard's gamma ray is given by the following equation.

$$E(e_i) = \frac{I_{e_i} (e^{\lambda_{e_i} t})}{I^o_{e_i}}$$

where $E(e_i)$ is the detector efficiency at the energy e_i

I_{e_i} is the measured photopeak area of the standard's gamma ray at the energy e_i in counts/minute.

$e^{\lambda_{e_i} t}$ is the factor for the correction of the photo-peak intensity to what it would have been on

the date the source was calibrated, based on

the decay constant λ_{e_i} for the source nuclide

and the time elasped, t, since the calibration

date (January 1, 1968).

$I_{e_i}^o$ is the absolute disintegration rate in counts/

minute for the standard source's gamma ray on

the calibration date. This factor is a

product of the absolute disintegration rate

and the yield of gamma rays of energy, e_i, per

disintegration.

In Figure 5, a plot of the measured efficiency $E(e_i)$

at 10.0 cm above the detector is shown as a function of the

energy for each gamma ray of the standard sources. The

solid line represents a fourth degree polynomial function

in the energy that was fit to the experimental points by

use of a least squares polynomial approximation computer

method called OPLSPA, a FORTRAN IV subroutine developed at

the ISU Computation Center (19). This function was used to

interpolate the efficiency of the detector between energies

of the standard source gamma rays. This efficiency curve

was then used to correct the photopeak intensities of the

^{190}Re gamma rays for the varying counting efficiency of the

Ge(Li) detector.

However, before this efficiency correction could be

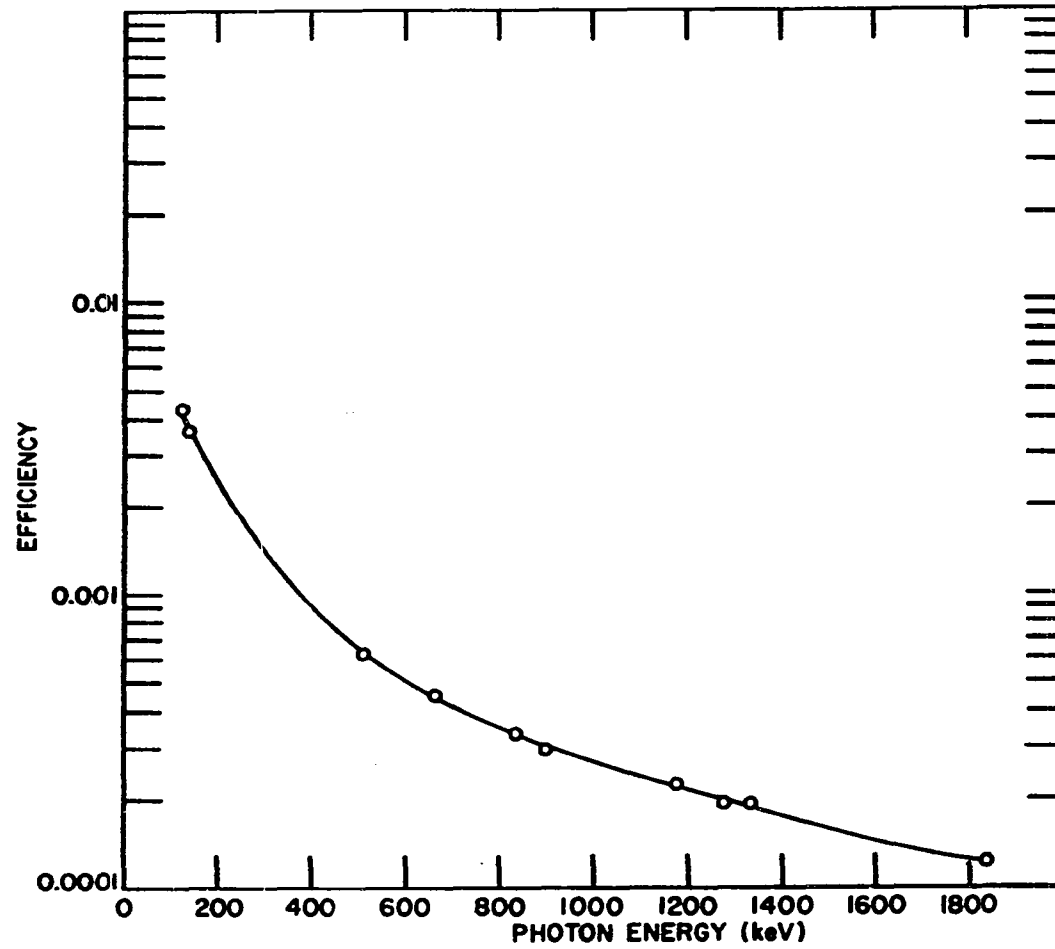applied to the photopeak intensities of the ^{190}Re transitions,

Figure 5. Efficiency curve of the Ge(Li) detector

an additional correction was required for the 187 and 361 keV lines. These two transitions occur in both the ^{190}Re and ^{190m}Os decays. Since both of these activities were present in the source, both activities contributed to the observed transition intensities. To correct the composite spectrum, Figure 1, for the presence of the ^{190m}Os lines, a spectrum striping correction was applied. This involved the subtraction of a spectrum due solely to ^{190m}Os (obtained by allowing all the ^{190}Re activity to decay before accumulation of the ^{190m}Os spectrum) from the composite ^{190}Re - ^{190m}Os spectrum. A spectrum striping computer routine (20) which fit the 615 keV line in the pure ^{190m}Os spectrum to the 615 keV line in the composite spectrum was used to calculate the fraction of the ^{190m}Os contribution to the composite spectrum. Either the 615 or 502 keV lines of ^{190m}Os could have been used, since both were due solely to ^{190m}Os. However, the somewhat better resolved 615 keV line was used instead of the 502 keV line which was partially overlapped by the 511 keV line caused by the decay of positron-emitting surface contaminants on the Os metal powder. The corrected spectrum representing only the gamma ray lines due to ^{190}Re was then analyzed by the ICPEAX program, followed by the efficiency and transition intensity normalization procedures described above. The normalized gamma ray intensities for ^{190}Re

31

are shown in Table 5. The uncertainties are based on the standard deviations of the photopeak fits performed by the ICPEAX program.

Table 5. Normalized gamma-ray transition intensities for ^{190}Re

Energy	Intensity	
186.9 keV	237 $\pm$ 30	
199.3	weak	
224.1	100	12
361.4	125	25
371.5	115	10
397.4	51	5
407.3	81	10
431.7	85	10
557.7	182	15
469.1	130	12
605.3	80	10
630.6	85	10
768.9	weak	
828.9	142	15
838.8	28	10
1200.3	weak	
1387.7	weak	

D. Construction of the Decay Scheme

Once the energies and intensities of the gamma-ray transitions of the ^{190}Re decay had been measured, a partial decay scheme was constructed. Although the investigation of the ^{190}Re decay was attempted in an effort to provide new information on the energy level structure of ^{190}Os, it quickly became clear that the ^{190}Re decay was in fact occurring to previously characterized levels of ^{190}Os and that the subsequent gamma-ray transitions did not excite any previously unobserved states in ^{190}Os. However, the 432 keV transition in the ^{190}Re decay appeared to indicate a new depopulation mode for one of the previously observed ^{190}Os excited states.

Actual construction of the gamma-ray portion of the decay scheme was greatly facilitated by the substantial information previously published about the ^{190}Os levels (8, 9,10). This nucleus has been intensively studied by various nuclear spectroscopic techniques. All of the observed ^{190}Re gamma rays were placed in a decay scheme based on previously reported excited states of ^{190}Os. All of the ^{190}Re gamma rays except the 432 keV transition are identical to transitions in the ^{190}Ir → ^{190}Os decay. This partial decay scheme is shown in Figure 6. Only those levels populated in the ^{190}Re decay are shown. The energy level spins and parities for the ^{190}Os states are those of

33
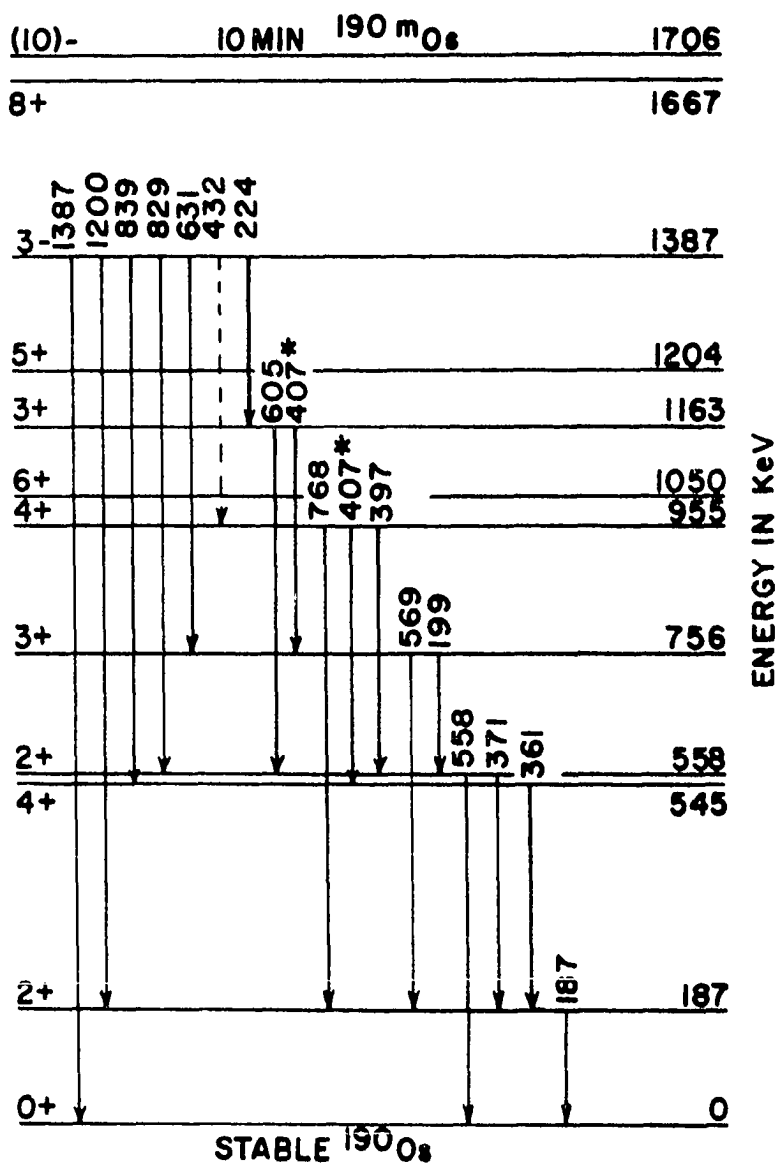
* INDICATES TWO TRANSITIONS WITH EQUAL ENERGIES

Figure 6. Partial gamma-ray decay scheme for ^{190}Re

Mariscotti (9). The ^{190}Re gamma-ray energies fit into this
energy level scheme without requiring significant changes
in the excitation energies for the levels. Solely on the
basis of energy, the 432 keV transition appeared to connect
the 1387 and 955 keV states. This initial placement in the
decay scheme was subsequently confirmed by the observation
of the same transition in the ^{190}Ir decay and by coincidence
measurements described below.

Following the conclusion of the ^{190}Re work, other workers
(21) observed the same transition in the ^{190}Ir decay. Two
additional features of the gamma-ray portion of the decay
scheme were evident. The apparently single transitions at
407 and 199 keV had previously been recognized as double
transitions between two pairs of ^{190}Os levels each (8). In
the case of the 407 keV line, the two transitions are
extremely close in energy; the gamma-ray spectra showing no
evidence for doublet lines. On the other hand the 199 keV
line is caused by two transitions which have a somewhat
greater difference in energy. The fairly large uncertainty
in the energy assigned by the ICPEAX program for the 199 keV
transition indicated the probable presence of a doublet
pair of lines, incapable of being resolved. The second
feature concerns the lack of any beta- or gamma-ray decay
to the four recently observed new levels in ^{190}Os below the
1387 keV state. None of the three levels at 912, 1115, and

1384 keV seen by Mariscotti (9) or the 840 keV level observed by Casten (10) is involved in the ^{190}Re decay. This is probably to be expected since these levels were not observed in studies of the ^{190}Ir (8) decay which populated states in ^{190}Os in a manner somewhat analogous to the ^{190}Re decay.

From the gamma-ray cascade pattern shown in Figure 6, and on the basis of the gamma-ray transition intensity measurements, it is obvious that the 1387 keV level is strongly fed ($\sim$ 100 percent) by the ^{190}Re beta decay. In an attempt to deduce the amounts (if any) of beta feeding to the other ^{190}Os levels, calculations were made to check the consistency of the gamma-ray feeding and decay for each of the ^{190}Os levels involved in the decay scheme. In some cases this could easily be done, since the multipolarities of the transitions and their internal conversion coefficients had been previously measured (22). However, internal conversion coefficients for several of the transitions had not been measured. This prevented accurate checks on the ^{190}Os levels either fed by these transitions or depopulated by them. Also the unresolved 199 and 407 keV doublet lines prevented measurement of the fraction of transitions passing through the levels at 1163, 955, and 756 keV. A substantial number of the ^{190}Re gamma rays feed or decay from these states. It appears, despite these ambiguities, that the only satisfactory

explanation for the observed intensities of the ^{190}Re lines is the ~ 100 percent feeding of the 1387 keV level of ^{190}Os by the beta decay of ^{190}Re.

Beta spectra described below did not show any appreciable higher energy branches that would indicate any beta decay to levels below 1387 keV in ^{190}Os.

E. Beta Spectra

As discussed in the previous section, it was inferred that essentially 100 percent of the ^{190}Re beta decay was occurring to the 1387 keV level of ^{190}Os. Therefore if an accurate measurement of the ^{190}Re beta endpoint energy could be made, the spin and parity of the ^{190}Re ground state might be deduced from log $\underline{ft}$ calculations based on the ~ 100 percent beta decay branch, the measured ^{190}Re half-life, the spin and parity of the 1387 keV level. Two experimental problems would effect the accuracy and precision of such a beta endpoint energy measurement.

On the one hand, the low yields of the ^{190}Re activity from the synchrotron irradiations required the use of a high detection efficiency beta-ray counting device. The stilbene beta phosphor described earlier was such a detector, but its inherent poor resolving power made energy measurements possible only with modest precision. A high resolution beta-ray spectrometer utilizing magnetic field focusing of the beta particles would be of great advantage, but the need for

high activity sources and counting under vacuum conditions prevented its use.

On the other hand, the beta spectrum of the ^{190}Re sources would also contain contributions from the beta and internal conversion decays of the other radioactive products in the sources. The contributions from ^{191}Os, ^{191m}Os, and ^{190m}Os would be relatively insignificant since the beta decay energies were small and the internal conversion intensities were weak. However, the beta decay of 9.7 min ^{191}Re would represent a strong interference to the ^{190}Re beta endpoint measurement, since the ^{191}Re endpoint energy was approximately the same as that expected for ^{190}Re (18). Fortunately the difference in half-life between these two isotopes allowed the measurement of the ^{190}Re endpoint energy in a manner analogous to that employed in the case of the 10 min ^{190m}Os interference in the gamma ray spectra.

For purposes of energy calibration and resolution measurement, spectra of several beta ray and conversion electron standard sources were accumulated using the stilbene crystal. In Figure 7 is shown the beta and conversion electron spectrum of a standard ^{137}Cs source. The prominent photopeak is caused by internal conversion of the 2.3 min 661.6 keV state in ^{137}Ba that is fed by the ^{137}Cs beta decay. The energy, 624 keV, presents the difference between the transition energy (661.6 keV) and the K electron
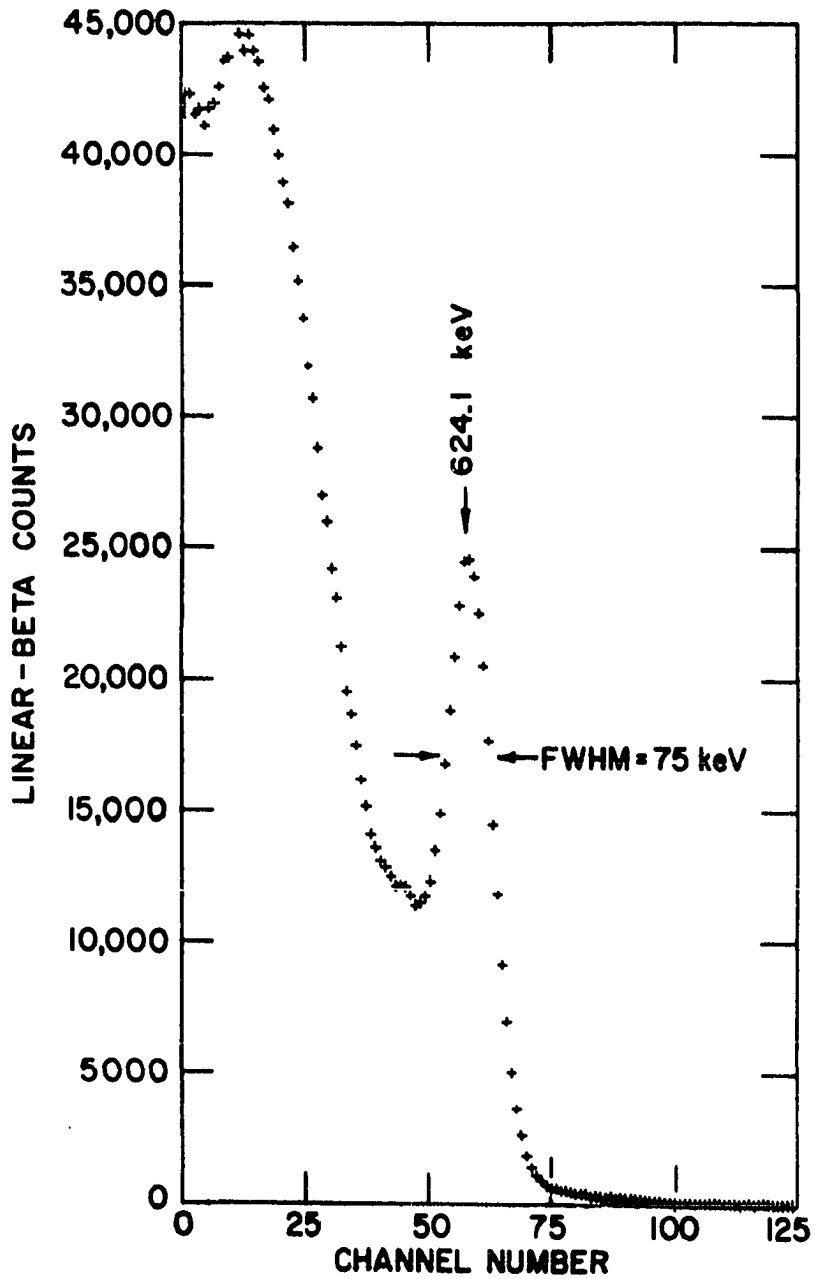
Figure 7. Beta ray and conversion electron spectrum
of 137Cs

binding energy (37.4 keV) in barium (23). As shown in the
figure the full width at half maximum resolution at 624 keV
was ~ 75 keV or about 12 percent. Similar spectra were
accumulated for ^{207}Bi to locate the conversion lines for
the 570 and 1060 keV transitions. These along with the
^{137}Cs measurement allowed a three point calibration line to
be made for the stilbene detector. As a check of the
counting systems general performance and the Kurie plot beta
analysis computer routine, spectra of ^{32}P, a pure, one
component beta emitting nuclide, were accumulated and
analyzed by the KURIE program. Sources of ^{32}P were prepared
by evaporating several drops of a ^{32}P solution on Mylar
film. These sources were counted as close to the detector
face as possible. In Figure 8 the beta spectrum of the ^{32}P
source accumulated in this manner is shown. The Kurie plot
analysis procedure incorporated in the KURIE program is
essentially that given by Siegbahn (24) with provisions for
corrections to the beta spectrum caused by finite nuclear
size and the acceleration of the beta particles by the nuclear
charge. The Kurie plot of the ^{32}P spectrum is shown in Figure
9 along with a visual estimate of 1.69 MeV for the endpoint
energy. This value compares favorably with the 1.71 MeV
endpoint energy quoted in the literature (25). Little if
anything can be said about the shape of the beta spectrum
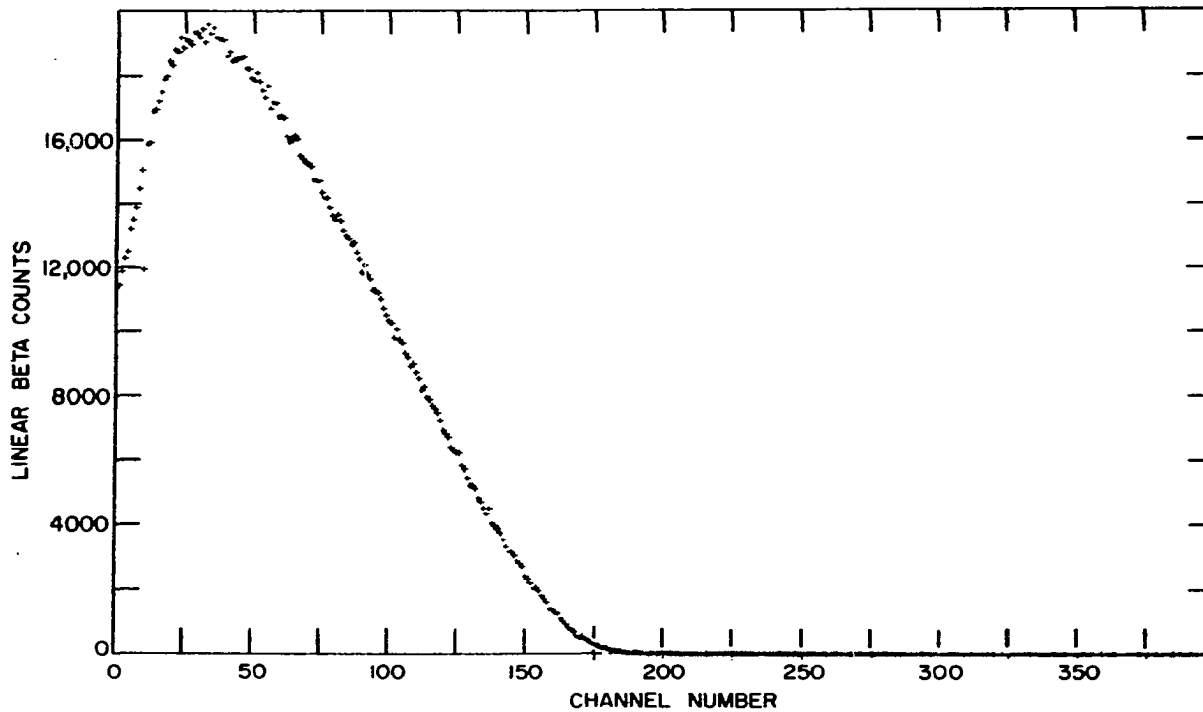since the variation of the detection efficiency was not known
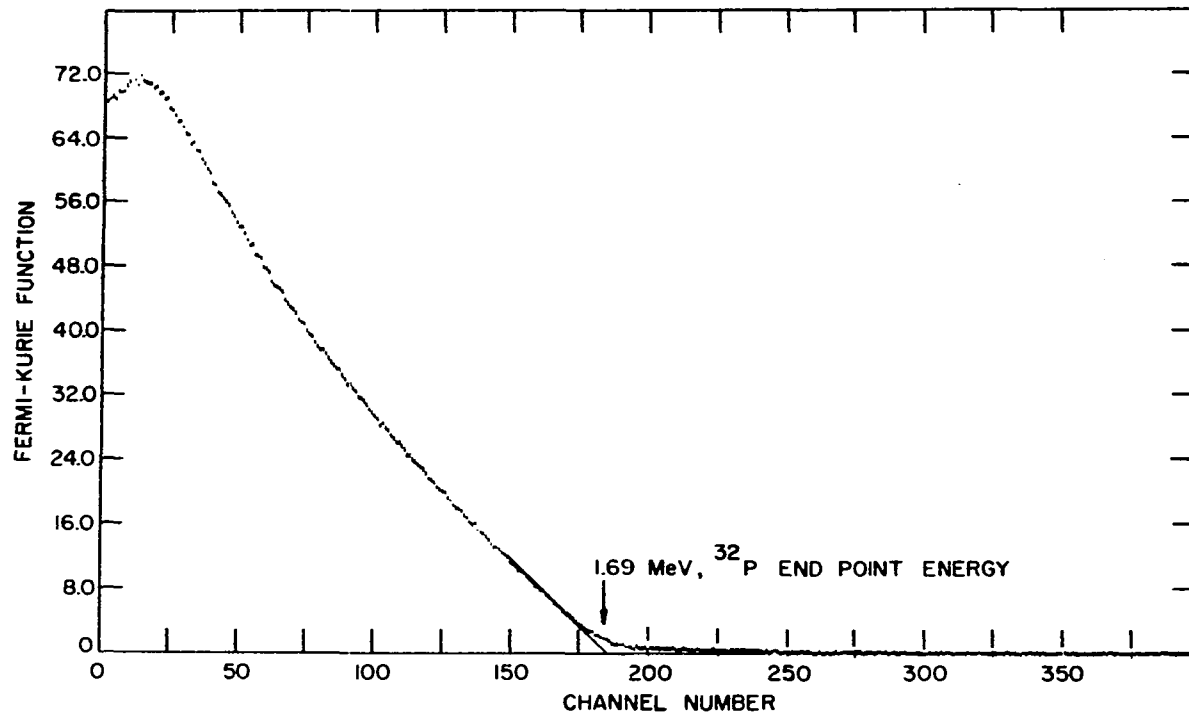
Figure 8. Beta ray spectrum of ^{32}P

Figure 9. Kurie plot of the ^{32}P beta ray spectrum

and could not be easily measured.

Measurement of the ^{190}Re beta spectrum was made using the counting techniques and computer analysis described above. Prior to counting, the synchrotron irradiated Os metallic powder was spread in a thin layer on the Mylar sheet and placed approximately 6 mm from the stilbene crystal face. A series of spectra was accumulated as the source activity decayed. Kurie plot analysis of these spectra revealed that the beta endpoint energy appeared to decrease with time. This was taken as an indication of the decreasing intensity for the ^{190}Re beta spectrum versus that for the long lived ^{191}Re and the presence of a higher energy beta endpoint for ^{190}Re than for ^{191}Re. Following the complete decay of ^{190}Re, the beta endpoint for ^{191}Re was measured to be 1.6 MeV, compared to 1.65 MeV predicted from semi-empirical mass equations (26). A spectrum taken 2.2 minutes after the end of the irradiation, Figure 10, showed a beta endpoint energy of 1.8 MeV which was taken to be the ^{190}Re value. This value compared favorably with the predicted value of 2.00 MeV based on an assumed 100 percent beta transition to the 1387 keV level of ^{190}Os (26). No experimental evidence was obtained for any significant beta branches to the ground or lower excited states of ^{190}Os.

Using this beta endpoint energy, the ~ 100 percent beta branch to the $I^{\pi} = 3^{-}$ level at 1387 keV in ^{190}Os and the
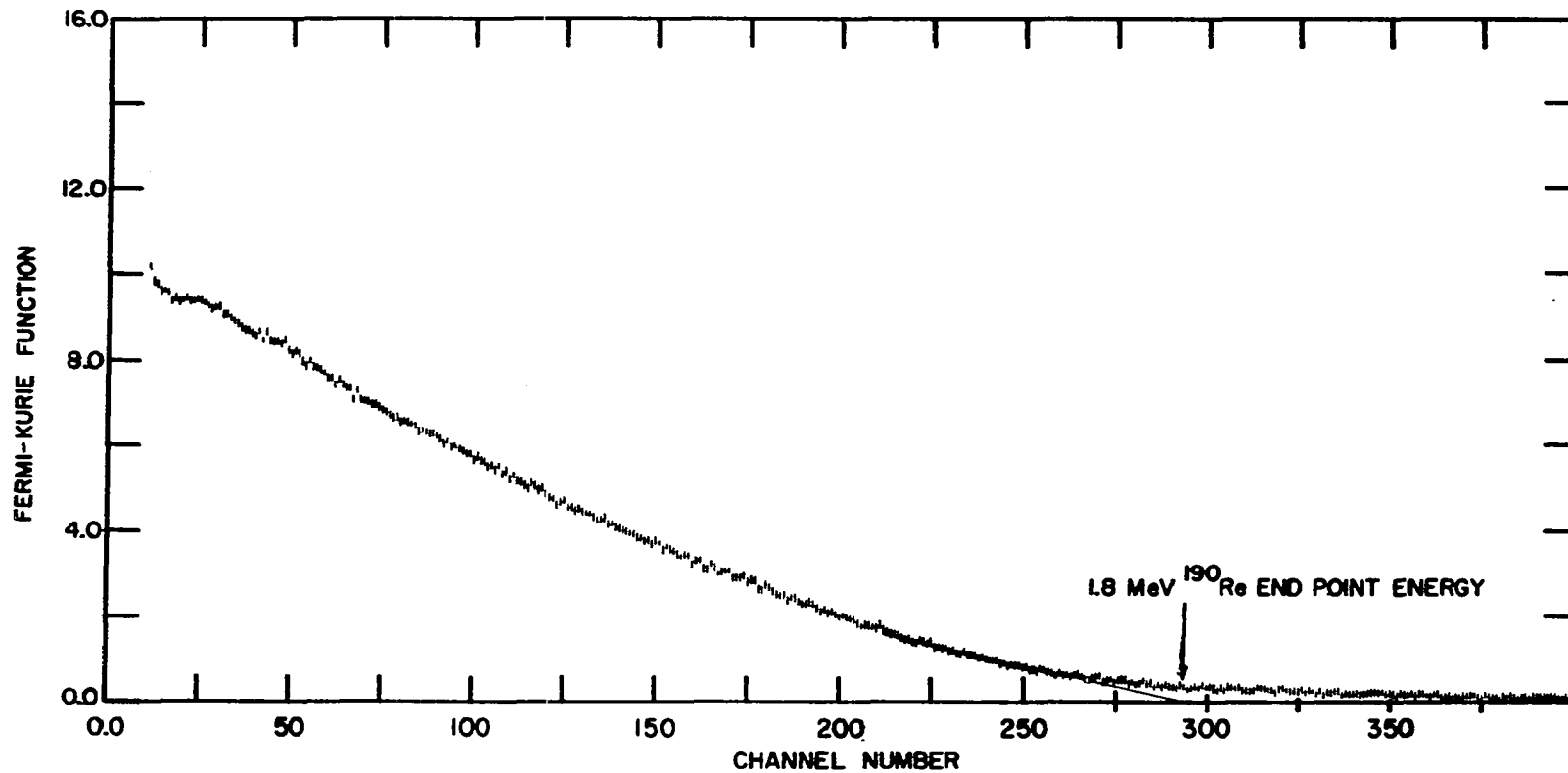
Figure 10. Kurie plot of the ^{190}Re source beta ray spectrum two minutes after the irradiation

measured ^{190}Re half-life, the log ft value of the beta

transition was calculated to be 5.1, using the standard log

ft calculation results of beta decay theory (27). This

value indicated a transition between states of the same

parity and differing in spin by no more than one unit of

angular momentum. Since the 1387 keV level has a spin and

parity of 3⁻ (9), the ground state of ^{190}Re would be of

negative parity and with nuclear spin of 2, 3, or 4.

F. Confirmatory Experiments

At this point in the investigation of the ^{190}Re decay,

the only feature which required additional study was the

proper placement of the 432 keV transition in the proposed

decay scheme. This section and the next describe the addi-

tional experimental work undertaken in completing this

feature of the decay scheme.

As mentioned earlier, it appeared that the 432 keV

transition connected the 1387 and 955 keV states of ^{190}Os,

based solely on the energy difference between these levels.

A number of investigations of the ^{190}Ir → ^{190}Os decay had

been reported in which gamma rays were observed depopulating

the 1387 keV level (8, 9). However in these studies, no

evidence was obtained for a 432 keV transition originating

at this level. This transition had however been previously

postulated as a decay mode for the 1387 keV state (8). It

appeared initially therefore that the 432 keV transition

must have a different origin. There is however a combination
of experimental relationships which could explain the failure
to observe the 432 keV transition in the ^{190}Ir decay. All of
the previous studies of the ^{190}Ir $\rightarrow$ ^{190}Os decay have been
made utilizing conversion electron spectroscopy. Previous
investigators realized that the complexity of the decay
scheme for ^{190}Ir prevented its elucidation using gamma-ray
spectroscopy and low resolution NaI(Tl) detectors. Since
these investigations were made before the availability of
high resolution Ge(Li) detectors, the only satisfactory method
for studying the decay was by means of internal conversion
spectroscopy which provided sufficient resolution for a decay
scheme of the complexity under study. The bulk of the ^{190}Ir
decay scheme was constructed based on such work. This tech-
nique, like various others, can be insensitive to particular
transitions. If a transition is of the strongly allowed
gamma-ray type (E1, M1, E2, etc.) the fraction of the decays
occurring by the alternate internal conversion mode will be
small and more difficult to detect using internal conversion
spectroscopy. It should be noted that if the 432 keV
transition were properly placed as proposed, it would be
predominately E1 in type. Moreover, if the transition
originates from an excited nuclear state that is only weakly
fed, the detection probability for the transition is addi-
tionally decreased relative to transitions occurring from

strongly fed states. These two situations, in fact, occurred in the ^{190}Ir decay and prevented the detection of the 432 keV transition from the 1387 keV level. Gamma-ray spectroscopy however, utilizing the now available Ge(Li) detectors, would provide a much more sensitive detection method for such a transition. It was for these reasons that a source of ^{190}Ir was prepared and used with a Ge(Li) detector to accumulate its gamma-ray spectrum.

The source of ^{190}Ir was prepared by a 13.5 hr irradiation of ~ 75 mg of powdered iridium metal of natural isotopic distribution. Reactions of the type (γ, n) were observed to predominate yielding 72 day ^{192}Ir and the ground and double isomeric states of ^{190}Ir as the primary reaction products. The decay scheme of ^{192}Ir (28) is sufficiently simple that it caused no difficulty in the gamma ray spectroscopy that followed the irradiation. The source was not counted immediately after the irradiation however. Since one of the ^{190}Ir isomeric states is beta active and both are short lived compared to the 12 day ^{190}Ir ground state, a cooling period following the irradiation would serve two purposes. The decay of the isomeric states to the ground state would maximize the yield of the ground state since it was longer lived than either of the states feeding it. Also the complete decay of the beta active isomer would eliminate the confusion as to which state is populating the excited ^{190}Os levels.

The gamma-ray spectrum of the ^{190}Ir source several days
after the irradiation is shown in Figure 11. A 432 keV
gamma-ray line is clearly evident in the spectrum along with
others at 224, 631, 829, 839, 1200 and 1387 keV known to
be depopulating the 1387 keV level of ^{190}Os. The relative
intensity of the 432 keV line compared to other transitions
in the ^{190}Ir decay was observed to remain constant over a
period of several ^{190}Ir half-lives, indicating that the 432
keV transition was in fact part of the ^{190}Ir decay. Of even
greater importance however, was the fact that the relative
intensities of the gamma rays depopulating the 1387 keV
level (including the 432 keV line) were the same, within
experimental error, for both the ^{190}Re and ^{190}Ir decays.
In Table 6 these relative intensities are shown. These
experimental results strongly indicated the correct place-
ment as proposed for the 432 keV transition. The next
section presents a discussion of two additional measurements
of the 432 keV transition in the ^{190}Re decay which confirmed
the correct placement of this transition.

G. The 432 keV Transition in the ^{190}Re Decay

The results of the ^{190}Ir confirmatory experiments
described above were strong evidence for the correct place-
ment of the 432 keV transition as proposed in the ^{190}Re
decay scheme. It was felt however that additional evidence
for this placement should be obtained directly from the ^{190}Re
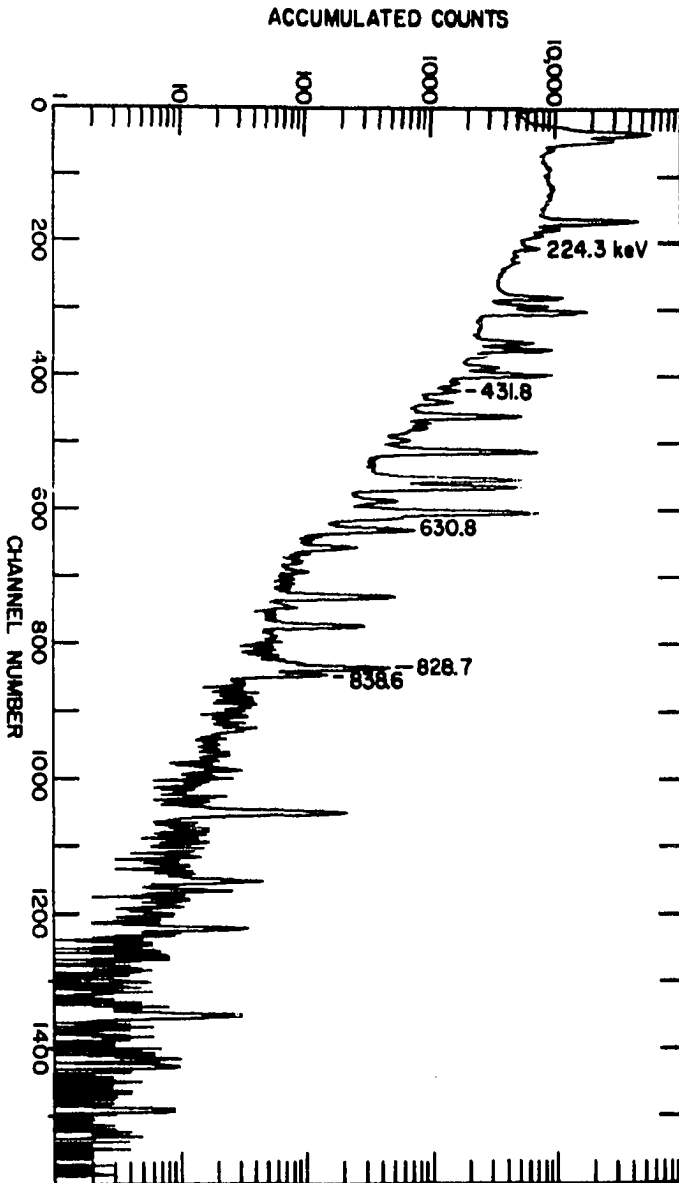
Figure 11. Gamma ray spectrum of the 190Ir source

Table 6. Comparison of the relative gamma-ray intensities
from the 1387 keV level of ^{190}Os fed by ^{190}Re
and ^{190}Ir

E_γ keV	^{190}Re	^{190}Ir
224	100 ± 12	100 ± 8
432	85 ± 10	89 ± 10
631	85 ± 10	109 ± 15
829	142 ± 15	140 ± 15
1199	weak	11 ± 4
1387	weak	weak

decay in addition to that already obtained from the ^{190}Ir

experiments. As a consequence, two additional studies were

made of this transition and are described in this section.

Measurement of the apparent half-life for the 432 keV

transition was first made in an attempt to show that this

transition followed the ^{190}Re ground state half-life. The

spectrum multiscaling mode of the 1600 channel analyzer

allowed time sequenced accumulations of the gamma-ray spectra

to be sored in 16 groups of one hundred channels each in the

analyzer's memory. The counting system was adjusted so that

the 432 keV photopeak would fall in the middle of the 100

channel subgroups. A source of ^{190}Re was prepared in the

usual manner and counted using the above technique starting
2 minutes after the irradiation for a period of 16 minutes.
The 432 keV photopeak in each of the 16 spectra was inte-
grated, and the area plotted on a semi-log axis versus time
to yield the decay curve for the transition. This plot is
shown in Figure 12. A linear fit to the data points was
made visually which indicated a half-life of 3.4 $\pm$ 0.3
minutes for the 432 keV transition. This agreed fairly well
with previous measurements of the ^{190}Re half-life and
indicated that the transition was part of the ^{190}Re decay.

The final measurement designed to confirm the correct
placement of the 432 keV transition involved gamma-gamma
coincidence counting of the ^{190}Re source. A coincidence
circuit utilizing the dual analog-to-digital converters of
the analyzer and Ge(Li) and NaI(Tl) detectors was set up to
accumulate the spectrum of the ^{190}Re gamma rays in coincidence
with the 432 keV transition. The Ge(Li) detector was gated
to count the 432 keV transition and to trigger the coincidence
circuit so that the 3 inch NaI(Tl) crystal could detect the
gamma rays in coincidence with this transition. The two
detectors were arranged with an angle of 90° between them
and positioned so that the source would be approximately
2.5 cm from either detector face. The coincidence spectrum
from the NaI(Tl) detector, shown in Figure 13, was accumu-
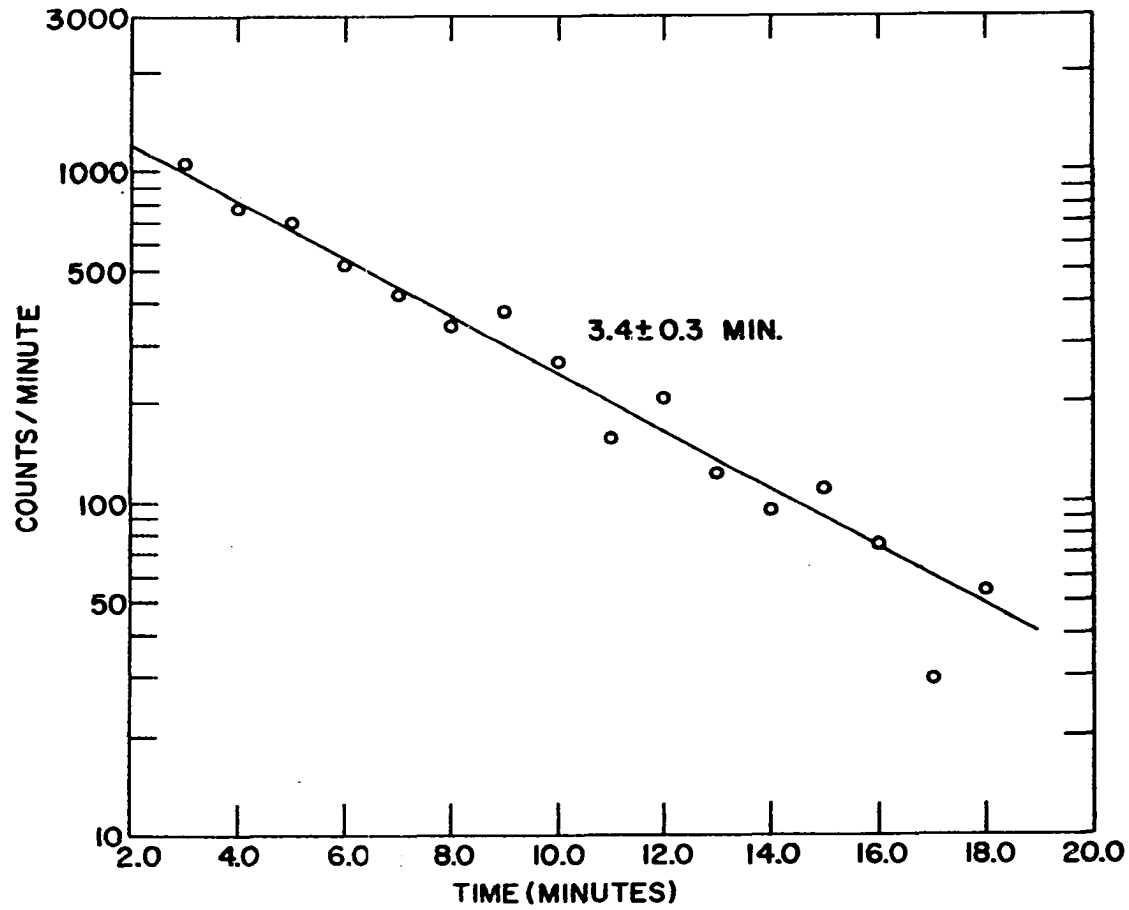lated by counting six sources of ^{190}Re which had been

Figure 12. Decay curve of the 432 keV transition in ^{190}Re

separately irradiated for 5 minutes and counted for three

minutes starting two minutes after the irradiation. If the

432 keV transition were properly placed as proposed, it

and subsequent transitions would populate excited ^{190}Os

levels at 955, 756, 558, and 548 keV which would in turn

decay by gamma rays with energies of 361, 371, 407, 558,

and 569 keV. The expected positions of these transitions

in Figure 13 are indicated by arrows. The rather broad

photopeaks immediately under these arrows indicate that, in

fact, the expected transitions have been detected and the

proposed placement of the 432 keV transition between the

1387 and 955 keV levels of ^{190}Os is correct.

H. Discussion of the Experimental Results

In Figure 14 the final proposed decay scheme for ^{190}Re

is shown, based on the experimental work described in the

previous sections. All of the known ^{190}Os levels below

1387 keV are shown even though some are not excited in the

^{190}Re, ^{190}Ir, or ^{190m}Os decays. The only levels above 1387

keV that are shown are the ones excited by the ^{190m}Os decay.

The spin and parity assignments are those of Mariscotti

et al. (9).

Once the decay scheme for the 3.1 min ^{190}Re activity

had been determined, attempts were made to observe the 2.8 hr

^{190m}Re isomeric state reported by Baro and Flegenheimer (7).

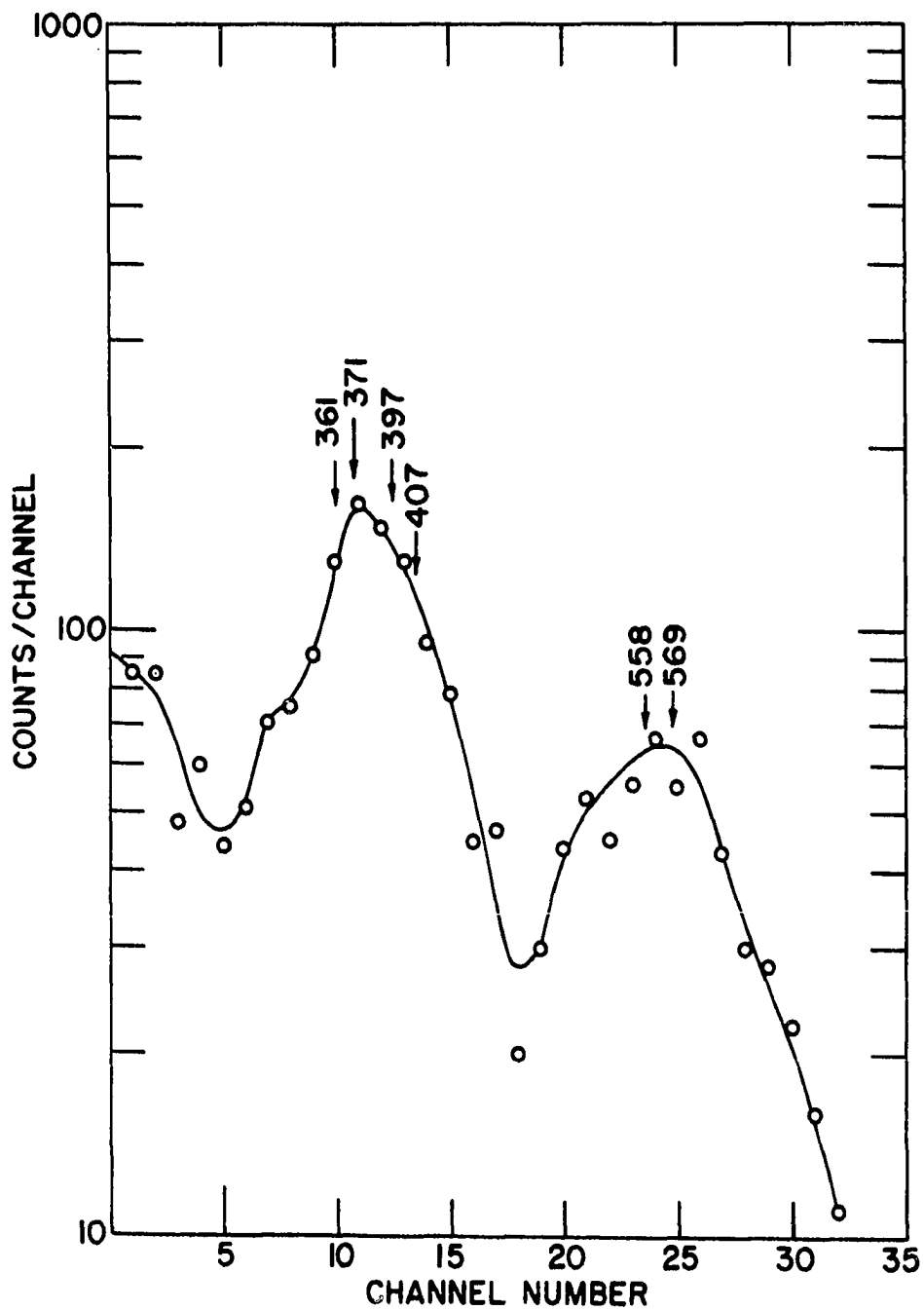Synchrotron irradiations of up to 2 hours duration were made

Figure 13. Gamma-gamma coincidence spectrum gated by
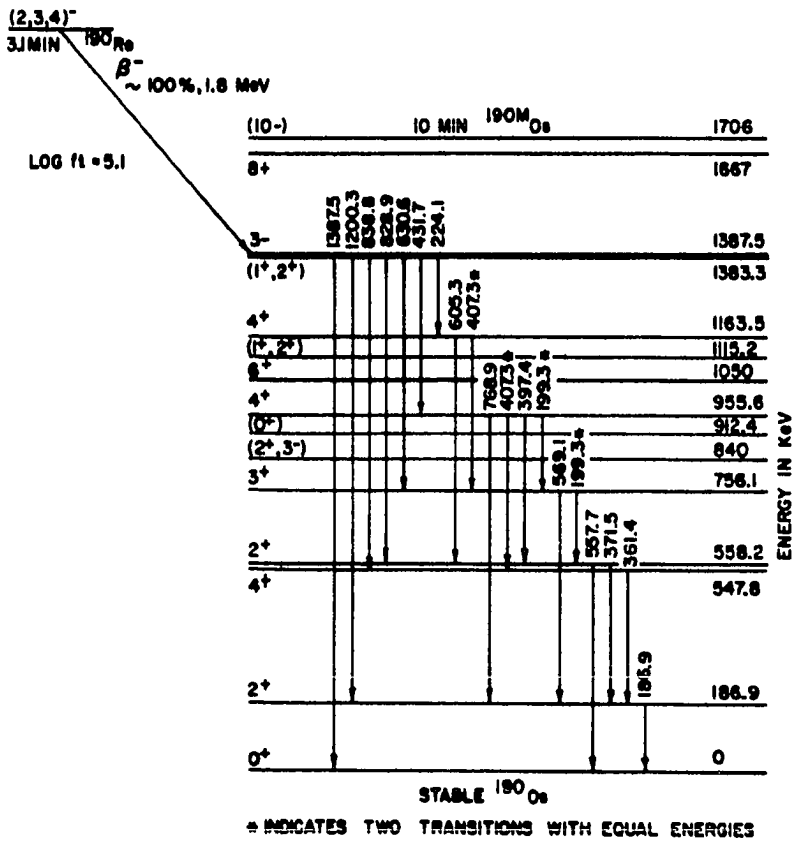the 432 keV transition

Figure 14. Proposed decay scheme for 3.1 min ^{190}Re

on the isotopically separated ^{192}Os targets. Gamma-ray
spectra accumulated using the Ge(Li) detector failed to show
any lines corresponding in energy to those ascribed to ^{190m}Re.
In fact all the lines present in the spectrum could be
assigned to products seen in the previous work. This fact
also discounted the possible production of ^{190}W and its
decay to ^{190m}Re. Gross beta- and gamma-ray multiscaling
also failed to show any additional long lived ($\sim$ 2.8 hr)
decay component. It appeared therefore that either the 2.8
hr activity observed by Baro and Flegenheimer (7) was in-
correctly assigned to ^{190}Re or that the photoproduction of
this isomeric state in ^{190}Re was quite low. It should be
noted that if the isomeric state in ^{190}Re has a high spin,
its production would be small since the target, ^{192}Os, is
an even-even nucleus with spin equal to zero.

Following the conclusion of the work on the ^{190}Re
decay, a paper by Yamazaki, Ikegami, and Sakai (21) appeared
describing a study of the ^{190}Ir $\rightarrow$ ^{190}Os decay. The investi-
gators used Ge(Li) detectors to accumulate the gamma-ray
spectrum of ^{190}Ir. They observed the same 432 keV transi-
tion that was seen in this investigation and independently
placed it between the same two excited ^{190}Os levels as has
been proposed here. In addition, Yamazaki et al. (21) made
gamma-ray angular correlation measurements and deduced from
these the spin and parities of several ^{190}Os levels. Their

decay scheme for transitions between levels at or below 1387 keV in ^{190}Os agree with the ones presented here.

Discussion of features of the ^{190}Re decay and their relationships to theoretical nuclear models is given in the next section.

V. THEORETICAL DISCUSSION

The osmium nuclei span one of the regions of nuclear structure in which changes from spherical to deformed nuclear shape occur. The energy level structure of ^{190}Os suggests that it is part of this deformed group of nuclei. A number of nuclear models have been presented to explain the properties of these deformed nuclei (29, 30, 31). This section attempts to discuss the experimental results within the framework of these models without resorting to elaborate theoretical arguments.

Nuclear models for the deformed even-even nuclei begin with the representation of the nuclear surface in terms of spherical harmonic expansions using Y_{2m} functions for positive parity energy levels and Y_{3m} functions for negative parity energy levels. Rotational and vibrational degrees of freedom of the deformed nuclear surface are assumed to be present, and that these processes give rise to the observed excited state spectra of these nuclei.

Predictions of these models include the existence of a rotational band built upon the ground state as a band head with spin changes of two units of angular momentum between adjacent levels. In the ^{190}Os nucleus these levels occur at 0, 186.7, 547.8, 1050, and 1662 keV with spins and parities of 0^+, 2^+, 4^+, 6^+, and 8^+ respectively. Rotational bands of this type are typically observed to obey the

following energy eigenvalue equation: $E_J = (\hbar^2/2I)$ $J(J + 1)$, where E_J is the energy of the level with spin J, $\hbar^2/2I$ is the usual rotational constant, and J is the spin of level in units of $\hbar$. An additional feature of these models is the prediction of other rotational bands built upon vibrational excited states. The ^{190}Os levels at 558.2, 756.1, and 955.6 keV with spins and parities of 2^+, 3^+, and 4^+ respectively appear to be the first three members of such a vibrational-rotational band. From these data it is possible to calculate the rotational moments of inertia and the quanta of vibrational energy in each band.

The beta decay of ^{190}Re unfortunately occurs to one of the lower lying excited states of ^{190}Os and therefore does not provide information about excited states of ^{190}Os above 1387 keV. Consequently tests of the predictions made by the nuclear models mentioned above are somewhat restricted to those specific cases involving the rotational bands of the ground state and first excited vibrational states which occur below 1387 keV.

A number of workers have attempted to describe the fairly large number of ^{190}Os states that are now known. The reader is referred to these discussions for additional material (32,33,34).

VI. FUTURE WORK

The quite short half-life of the ^{190}Re ground state and the low synchrotron yield of this activity from ^{190}Os targets greatly restrict the number of nuclear spectroscopic techniques which can be applied to the study of this decay. The foregoing material represents the results of experimental techniques of modest sophistication that were applicable to this situation. A number of refinements to the proposed decay scheme might be made following further experimental work suggested below.

The existence of additional beta branches from the ^{190}Re ground state might be detected by more sophisticated beta-ray counting and analysis. Plastic scintillation detectors might be of use for such a study. If high activity sources of ^{190}Re could be prepared, perhaps by the reactions used by Aten (6) rather than synchrotron activation, it might even be possible to employ a magnetic focusing beta ray spectrometer for not only beta ray measurements but also conversion electron studies of the ^{190}Re gamma-ray transitions.

In the final analysis, high specific activity ^{190}Re sources are necessary to counteract the unfavorably short half-life of this activity. If such sources could be obtained in the future, continually improving nuclear spectroscopic equipment and techniques could be used to refine all aspects of the decay scheme for ^{190}Re.

PART II. ISOMER RATIO MEASUREMENTS

IN PHOTONUCLEAR REACTIONS

VII. INTRODUCTION

A. History and Importance of Isomer
Ratio Measurements

The correlations between experimentally deduced nuclear
properties and the theoretical features of various models
for nuclear structure have provided the justification and
motivation for continued study of nuclear systems both
theoretically and experimentally. The measurement and inter-
pretation of nuclear reaction cross sections has been one area
in which significant information about nuclear structure and
reaction mechanisms has been obtained. Following the dis-
covery of the phenomenon of nuclear isomerism (35), it was
pointed out that measurements of the reaction cross sections
(or their ratio) for the formation of nuclear isomeric and
ground state pairs could yield detailed information about
the energy level structure of the product nucleus and the
angular momentum, energy, and reaction mechanism effects
that control the cross section ratios (36).

Nuclear reactions induced by high energy photon bombard-
ment are of particular usefulness in studies of this type.
Photoactivation resulting in the emission of a few nucleons
can be interpreted successfully when viewed as the absorption
of low multipolarity (usually El) photons, followed by
nucleon emission from the excited compound nucleus (37).

In the case of isomeric pair states in the product

nucleus, most of these measurements have involved the bombardment of nuclei with high energy photons and the detection of radiations from the ground and isomeric states to determine the cross sections for the production of these states. When products from (γ,n) or (γ,p) reactions on even-even nuclei were studied, the state with lower spin was observed to be populated more frequently (38). This observation seemed consistent with the notion that the compound nucleus would have a spin and parity of 1^-, corresponding to the absorption of El photons by the even-even target nucleus with spin and parity of 0^+. The compound nucleus would then emit a nucleon and perhaps one or more gamma rays before decaying to one or the other of the isomeric pair states. Since the emission of low orbital angular momentum (usually $l = 0$) nucleons and low multipolarity gamma rays is favored over higher angular momentum processes, the state with lower spin would be favored.

This view of the photonuclear activation of isomeric pair states has been the starting point for many experimental and theoretical studies. The work described in this part of the thesis concerns an extension of this subject.

B. The Present Study

The bulk of the work done previously on the measurement and interpretation of photonuclear isomeric pair production cross sections (or more simply isomeric pair cross sections

or isomer ratios) has concerned reactions in which one
nucleon (usually a neutron) is emitted from the target
nucleus. These studies have been conducted with a variety
of target nuclei and counting equipment, over wide energy
ranges (39, 40).

Little information however has been reported for cases
in which an isomeric pair of states in a particular nucleus
has been produced by more than one type of reaction. It was
thought that studies of this type would be useful, in that
the measurements of the isomer ratios for each reaction
could indicate whether the simple model described earlier
would successfully explain situations of greater complexity
than those simple cases already observed. In particular, it
appeared possible to measure the isomer ratios for several
nuclei that could be produced by both (γ,n) and (γ,3n)
reactions with stable isotopes one or three neutrons richer
than the isomeric pair nucleus. Thus by irradiation of
isotopically separated targets and by following the decay
of the ground and isomeric states in the product nucleus,
one could determine the isomer ratio (or yield ratio as was
the case in this study) for both the (γ,n) and (γ,3n)
reactions. These measurements could then be used to evaluate
the validity of the photoactivation mechanism describing the
production of isomeric state pairs. Four cases were choosen
for the study: measurements of the isomer ratios for ^{91}Mo,

^{112}In, ^{137}Ce, and ^{141}Nd by the reactions (γ,n) and $(\gamma,3n)$ on the corresponding stable isotopes of these elements.

C. Literature Survey

This section deals with a survey of the literature as it pertains to two areas of the work presented in this portion of the thesis. The first part concerns the previously published decay scheme information of the activities that were produced in the synchrotron irradiations, and the second part surveys the previously published contributions of isomer ratio measurements in the same systems described here.

A search of the literature was made to obtain reports on the decay schemes of the ground and isomeric state activities in ^{91}Mo, ^{112}In, ^{137}Ce, and ^{141}Nd. The work of Cretzu, Hohmuth, and Schintlmeister (41) appeared to be the best effort to characterize the ^{91}Mo activities. Decay scheme parameters for ^{112}In were taken from the work of Ruan and Yoshizawa (42). The ^{137}Ce decay scheme information was obtained from the work of Frankel et al. (43). The report on the ^{141}Nd decay scheme by Kochler and Grissom (44) was used in connection with the decay of this activity. As a guide to the reader the pertinent decay scheme information for the ^{91}Mo, ^{112}In, ^{137}Ce, and ^{141}Nd activities are presented in Figures 15, 16, 17, and 18 respectively.
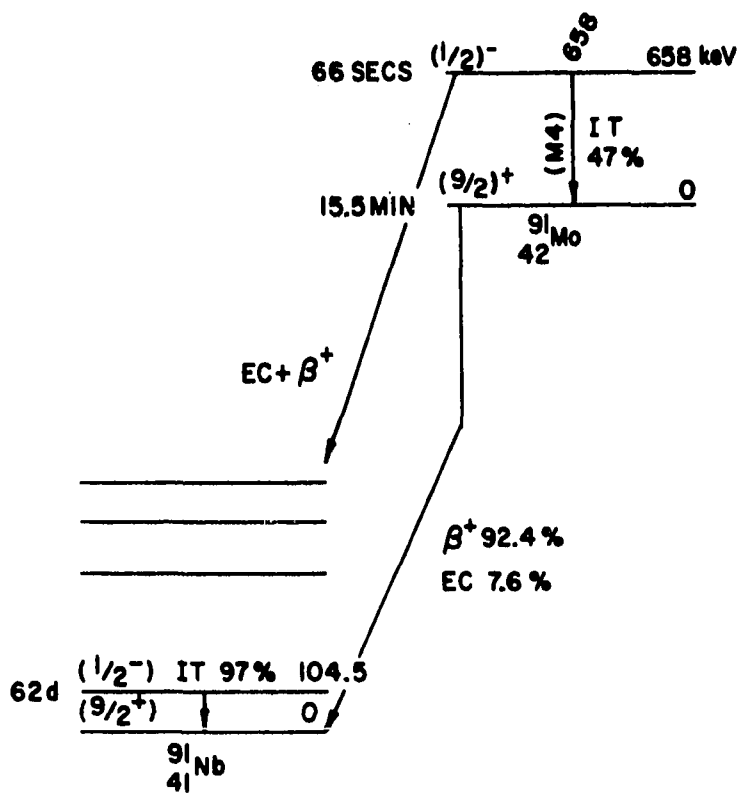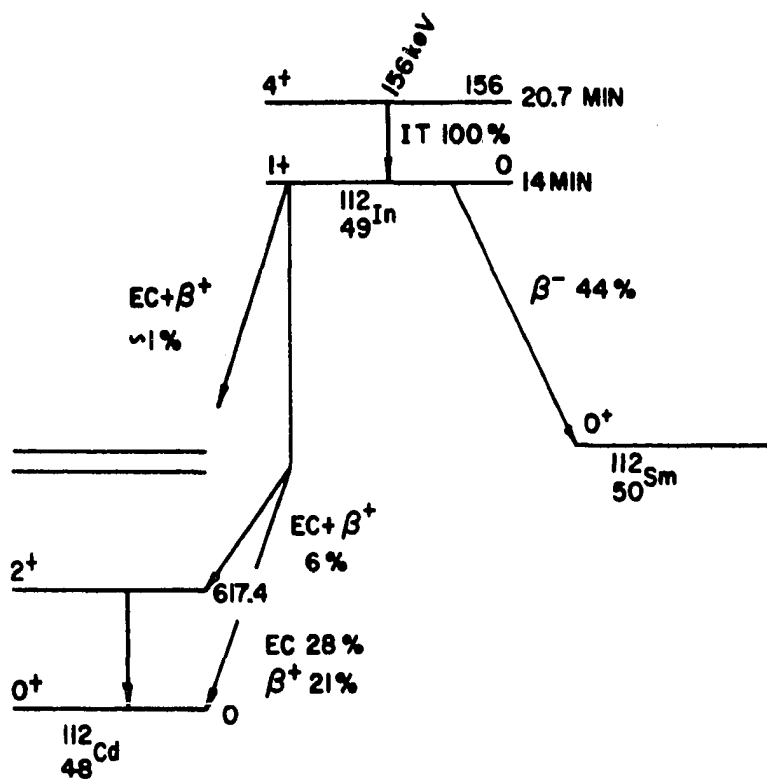
Figure 15. Decay scheme of ^{91}Mo

Figure 16. Decay scheme of ^{112}In
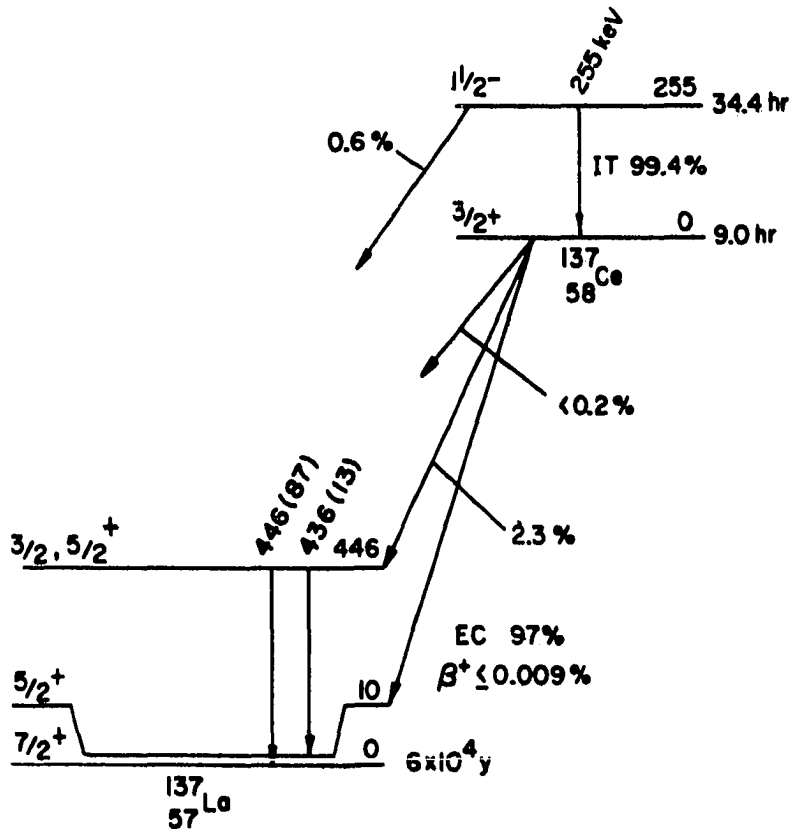
Figure 17.   Decay scheme of ^{137}Ce
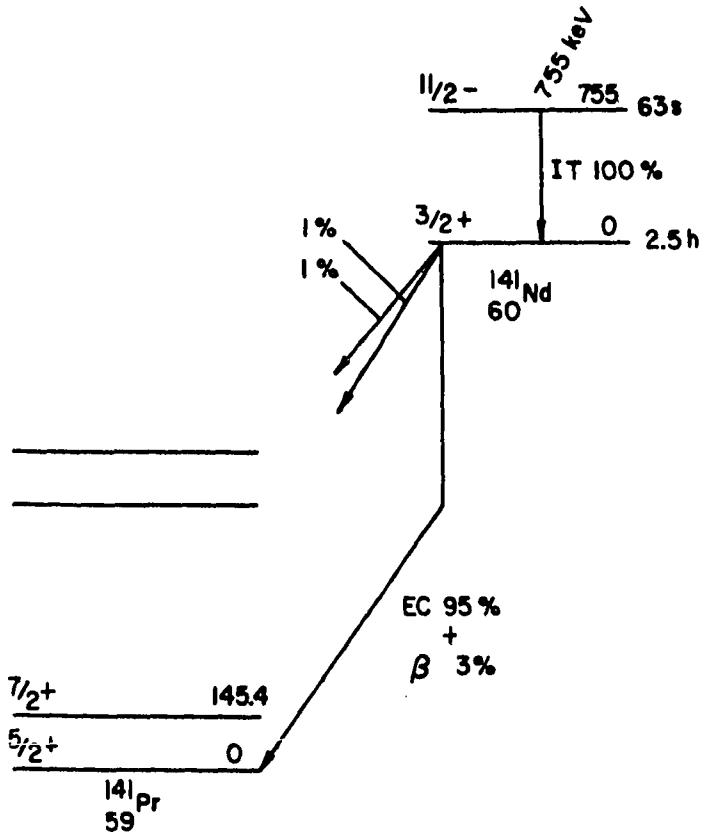
Figure 18. Decay scheme of ^{141}Nd

No information has been published concerning isomer ratio measurements from the same two reaction modes yielding the same final states in the systems which were studied in this investigation. Numerous reports of recent photonuclear cross section measurements and some isomer ratios have been summarized in publications of the International Atomic Energy Agency (39, 40). One pertinent report of the ^{92}Mo (γ,n)^{91}Mo reaction including isomer ratio measurements was found. Costa, Ferrero, Ferroni, Pasqualini, and Silva (45) measured the isomeric yield ratios as a function of energy up to 70 MeV and observed a greater yield for the low spin (1/2$^-$) ^{91}Mo isomer than for the higher spin (9/2$^+$) ^{91}Mo ground state for all energies above threshold.

VIII. OVERVIEW OF THE EXPERIMENTAL METHOD

The following section is an overview of the method and techniques used in the study of the isomer ratio measurements for these four systems. It is in three sections: the first dealing with the mathematical theory involved in the isomer ration measurements; the second with experimental considerations affecting the feasibility of performing the measurements; and the third section with a set of sample results and calculations to show how the data analysis was performed.

A. Mathematical Theory

The rate at which nuclear reactions occur when a particular target material is exposed to a flux of incident particles of sufficient energy to cause reactions is given by (46):

$$R = N \, \Phi \, \sigma \tag{1}$$

where

R = reaction rate, i.e., nuclei produced per sec,

N = number of target nuclei exposed to the flux,

Φ = flux of incident particles per cm^2 per sec,

σ = the reaction probability or "cross section" in cm^2.

In the case where synchrotron irradiation is used to

produce the reactions that are desired, the flux, Φ, varies with energy, corresponding to the nonmonoenergetic spectrum of photons produced by the accelerator. The cross section in general is also a function of energy. In this case Equation 1 is transformed into an integral over the energy range from the reaction threshold energy to the maximum energy of the accelerator.

$$R \; = \; \int_{E_{threshold}}^{E_{maximum}} N \, \Phi \, (E) \, \sigma \, (E) \, dE \tag{2}$$

If the product nuclei are radioactive and counted some time after the irradiation has ended, the disintegration rate of the product nuclei is given by (46):

$$D \; = \; R(1 - e^{-\lambda T_b})e^{-\lambda T_c} \tag{3}$$

where

D = product disintegration rate,

λ = product nucleus decay constant,

T_b = irradiation duration in time units,

T_c = time at which the counting was done as measured from the end of the irradiation.

The disintegration rate is then simply related to the number of product nuclei, N, at anytime by:

$$D \; = \; \lambda N$$

In the systems to be described later in this thesis, two radioactive states were produced in the product nuclei: the ground state and the isomeric state, lying several hundred keV in energy above the ground state. This situation is further complicated due to genetic relationships existing between these states. During the irradiation some of the product nuclei will be produced in their ground state and some in the excited isomeric state. It is precisely the ratio of these two reaction rates that is of interest. This ratio must be indirectly measured for the following reasons. Both during and after the irradiation some of those product nuclei in the isomeric state will decay partially, or in some cases totally to the ground state, thus increasing the total number of ground state product nuclei over those produced by direct reactions. During the same period of time, the ground state nuclei will themselves be decaying with their characteristic half-life. These processes are illustrated in Figure 19. The following radioactive decay equations given by Friedlander, Kennedy, and Miller (46) treat the situation described above.

$$D_1 = R_1(1 - e^{-\lambda_1 T_b})e^{-\lambda_1 T_c} \tag{4}$$

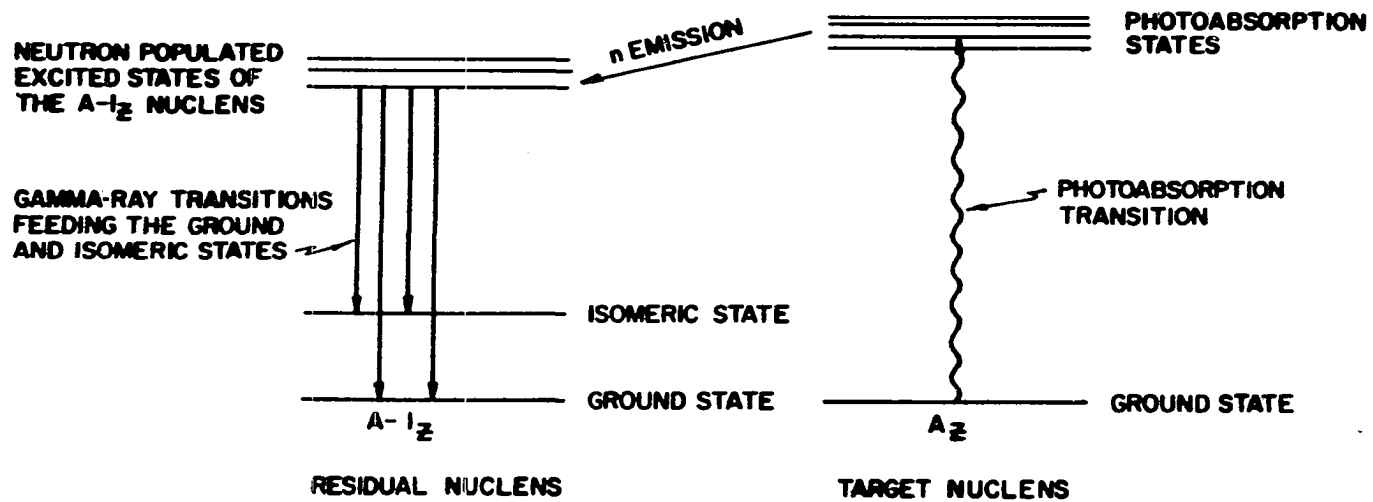$$D_2' = R_2(1 - e^{-\lambda_2 T_b})e^{-\lambda_2 T_c} \tag{5}$$

Figure 19. Schematic diagram of the reaction process

$$D_2'' = [PR_1(1 - e^{-\lambda_2 T_b}) + \frac{\lambda_2 R_1 P}{\lambda_1 - \lambda_2} (e^{-\lambda_1 T_b} - e^{-\lambda_2 T_b})]e^{-\lambda_2 T_c}$$

$$(6)$$

$$D_2''' = \frac{\lambda_2 PR_1(1 - e^{-\lambda_1 T_b})(e^{-\lambda_1 T_c} - e^{-\lambda_2 T_c})}{\lambda_2 - \lambda_1}$$

$$(7)$$

where subscripts 1 and 2 refer to the isomeric and ground states respectively. The factor P corresponds to the fraction of isomeric state decays that feed the ground state. Equation 4 is simply Equation 3 cast in terms of the isomeric state parameters. Equation 5 gives the disintegration rate of the ground state due to its production during the irradiation by direct reaction and its decay during and after the irradiation. The growth and decay of the ground state disintegration rate caused by the isomeric state's feeding of the ground state during the irradiation is given by Equation 6. Following the irradiation the isomeric state continues to decay and feed the ground state which also decays with its characteristic half-life. The disintegration rate due to this process is given in Equation 7.

Any measurement of the disintegration rates of the two states after the irradiation involves D_1 and the sum of D_2', D_2'', and D_2''', since only the sum of the ground state disintegration rates can be measured, not their origin. Once D_1 and the D_2 sum have been measured, the system of Equations 4

through 7 can be solved simultaneously for R_1 and R_2, the independent reactions rates for the two states.

This requires knowledge of the irradiation duration T_b, the cooling time before counting T_c, the decay constants λ_1 and λ_2 of the two nuclear states, the fraction of isomeric state decays to the ground state, P, and the relationship between the disintegration rate of the states and the activity observed with the detection apparatus. For the systems to be described later, this relationship is given by Equation 8.

$$D = A(1 + \alpha_T)(1/Eff)(1/F) \tag{8}$$

where

D   = absolute disintegration rate of the nuclear state,

A   = observed count rate in the detection apparatus,

α_T = total internal conversion coefficient for the gamma counted as characteristic of the nuclear state decay,

Eff = detection efficiency of the counting device for the gamma used to measure A,

F   = fraction of the decays of the nuclear state yielding gamma rays used to measure A.

Later in this section a set of sample calculations involving these radioactive decay equations will be illustrated for one of the systems studied.

B. Experimental Considerations

The following is a discussion of a number of experimental problems that had to be dealt with in the course of the work described below. They refer to the general experimental method that was used and are presented here rather than with the material pertaining to the individual systems.

The number of systems that can be studied by the method outlined previously is restricted by the necessary occurrence of several nuclear properties for the isotopes involved in the measurements. The primary requirement concerns the existence of nuclides with ground and isomeric states one and three neutrons poorer than two stable isotopes of a particular element. In addition the ground and isomeric states must have roughly comparable half-lives (in the range of seconds to hours). This insures that both states can be readily produced with relatively short synchrotron irradiations and counted after the irradiation without serious loss in accuracy and precision caused by the almost complete decay of the sample activity before the counting can be started. The decay schemes of the ground and isomeric states must be well characterized and include readily detectable radiations. Any additional activities induced in the target material must not act as interferences to the detection of the isomeric pair states.

For reasons explained more fully later, the two target

isotopes used to measure the (γ,n) and (γ,3n) isomer ratios must have the same spin and parity. In three of the four cases studied, the isomeric pair nucleus produced during the irradiation had an even number of protons and an odd number of neutrons. Consequently the target nuclides had both even numbers of protons and neutrons resulting in spins and parities of 0^+ for both. The ^{112}In system involved the ^{113}In and ^{115}In target nuclei which both have spins and parities of $5/2^+$ (42).

One can most readily measure the (γ,n) and (γ,3n) isomer ratios using pure isotopically separated targets of the two nuclides required. Unfortunately such materials are not yet available. Highly enriched target materials still contain small amounts of other mass isotopes in addition to the target isotope to be used. This problem is especially serious in the case of the A + 3 target isotope, where A is the mass of the isomer pair nucleus. Small amounts of the A + 1 target isotope in the enriched A + 3 material will yield comparable amounts of the isomeric pair activities because of the much greater (γ,n) photonuclear yield versus that for the (γ,3n) yield even with the enriched A + 3 target material. One can correct for this interference by using a flux monitor with the sample and by applying corrections to the yield data based on the reported isotopic composition of the target materials. Such calculations are

shown in the next part of this section.

C. Sample Calculations and Results

The material of this section illustrates the data
analysis procedure required to calculate the isomer yield
ratios which will be discussed later. The sample calculations
and results presented here are part of the molybdenum system
that is more fully covered in Section IX of this part of the
thesis.

Two samples of powdered molybdenum metal isotopically
enriched in masses 92 and 94 were separately irradiated along
with copper monitor foils in the synchrotron. Following the
irradiations the decays of the ground and isomeric states in
^{91}Mo were followed to construct decay curves of both
activities for evaluation of their half-lives and activities
as a function of time. The monitor foils were also counted
to measure the integrated flux or dose each sample received.
Previously published decay scheme information (41) for the
^{91}Mo activities was used to relate the observed count rates
to the absolute disintegration rates following corrections
made for the detector's varying counting efficiency. Table
7 summarizes the raw data for the ^{92}Mo and ^{94}Mo targets.
The calculations and results for the ^{92}Mo target are shown
below. The corresponding results for the ^{94}Mo target are
also shown along with the target impurity corrections.

Table 7. Data for isomer ratios for ^{91}Mo from targets of ^{92}Mo and ^{94}Mo

	^{92}Mo	^{94}Mo
Sample weight	0.3205 gm	0.6108 gm
Monitor weight	0.0285 gm	0.0291 gm
Irradiation duration	1.0 min	2.0 min

Half-lives measured
    Ground state
    Isomeric state
	16.25 min
	1.26 min
		16.0 min
		1.0 min

Observed activities
(Time after E.O.B.[a])
    Ground state
    Isomeric state
	10,000 cpm (32.75 min)
	10,000 cpm (3.40 min)
		1,000 cpm (32.00 min)
		800 cpm (2.73 min)

Monitor activity[b] at E.O.B.	45,200 cpm	60,000 cpm

Gamma-ray internal
conversion coefficients[c]
    Ground state
    Isomeric state
	0.0
	0.055
		0.0
		0.055

[a]E.O.B., End of bombardment.

[b]511 keV line of ^{62}Cu.

[c]Taken from reference (41).

Table 7. (Continued)

	^{92}Mo	^{94}Mo
% Isomeric decays to the ground state[c]	47.0	47.0
% of decays yielding gamma rays used to count[c,d]		
Ground state	184.72	184.72
Isomeric state	47.0	47.0
Counting efficiency at detector face		
Ground state (511 keV)	0.0153	0.0153
Isomeric state (658 keV)	0.0102	0.0102
Isotopic composition		
Mass number		
92	98.27	0.87
94	0.46	93.9
95	0.37	2.85
96	0.26	1.04
97	0.13	0.40
98	0.25	0.75
100	0.27	0.22
Atomic weight average	92.08	94.89

[d]Includes factor of 2 from positron annihilation.

1. <u>Sample calculations for the</u> ^{92}Mo <u>target</u>

Step 1: Conversion of the raw ^{91}Mo activities to absolute disintegration rates via Equation 8.

Isomeric state

$$10,000 \ (1 + 0.055)(1/0.0102)(1/.47) \ = \ 1.863 \times 10^6$$

Ground state

$$10,000 \ (1 + 0.0)(1/0.0153)(1/1.8472) \ = \ 3.534 \times 10^5$$

Step 2: Insertion of experimental and decay scheme parameters into Equations 4 through 7. Solve for $R1'_{92}$ and $R2'_{92}$. Subscripts refer to the target isotope, in this case ^{92}Mo.

$$1.863 \times 10^6 = R1'_{92} \ (1 - e^{-0.693(1.0)/1.26}) \ e^{-0.693(3.40)/1.26}$$

$$3.534 \times 10^5 = R2'_{92} \ (1 - e^{-0.693(1.0)/16.25}) e^{-0.693(32.75)/16.25}$$

$$+ \ .47R1'_{92} (1 - e^{-0.693(1.0)/16.25})$$

$$+ \ .47R1'_{92} (.693/16.25)/(.693/1.26 - .693/16.25)$$

$$x \ (e^{-0.693(1.0)/1.26} - e^{-0.693(1.0)/16.25})$$

$$x \ e^{-0.693(32.75)/16.25}$$

$$+ \ .47R1'_{92} \ (1 - e^{-0.693(1.0)/1.26})$$

$$x \ (e^{-0.693(3.40)/1.26} - e^{-0.693(32.75)/16.25})$$

$$R1'_{92} = 3.35 \times 10^7 \ ; \quad R2'_{92} = 1.71 \times 10^7$$

Step 3: Correction of the $R1'_{92}$ and $R2'_{92}$ to per mole Mo atoms basis and per unit of monitor foil activity per gram copper.

$$R1_{92} = R1'_{92} \ \frac{(0.0285)(1 - e^{-0.693(1.0)/10})}{4.52 \times 10^4 \ (0.320/92.08)}$$

$$= 407.7$$

$$R2_{92} = R2'_{92} \ \frac{(0.0285)(1 - e^{-0.693(1.0)/10})}{4.52 \times 10^4 \ (0.320/92.08)}$$

$$= 207.6$$

Similar calculations for the ^{94}Mo target yielded the following $R1_{94}$ and $R2_{94}$ values:

$$R1_{94} = 15.12 \ ; \quad R2_{94} = 9.05$$

Step 4: Correction of R1 and R2 values caused by target impurities.

The small ^{92}Mo impurity in the ^{94}Mo target material causes a problem at this point. The much larger yields of the ^{91}Mo activities from the ^{92}Mo target compared to the yields from the ^{94}Mo target indicate that the small ^{92}Mo

impurity in the ^{94}Mo material is responsible for a significant part of the yields of the ^{91}Mo activity when the ^{94}Mo target is irradiated. To compensate for this effect, the $R1_{94}$ and $R2_{94}$ values are corrected by subtracting weighted $R1_{92}$ and $R2_{92}$ factors based on the amount of ^{92}Mo in the ^{94}Mo material. The $R1_{92}$ and $R2_{92}$ values are assumed to represent the production of the ^{91}Mo states solely by the ^{92}Mo(γ,n) reaction. The final corrected R1 and R2 values are:

$$R1^{o}_{94} = [15.12 - (.0087)(407.7/.9827)]/.939 = 12.25$$

$$R2^{o}_{94} = [9.05 - (.0087)(207.6/.9827)]/.939 = 7.67$$

$$R1^{o}_{92} = 407.7/.9827 = 414.9$$

$$R2^{o}_{92} = 207.6/.9827 = 211.2$$

Taking the ratio of R1 to R2 for both targets yields:

$$\frac{R1^{o}}{R2^{o}} = \int_{E_{\text{threshold 1}}}^{E_{\text{maximum}}} N\Phi(E)\sigma_1(E)dE \Big/ \int_{E_{\text{threshold 2}}}^{E_{\text{maximum}}} N\Phi(E)\sigma_2(E)dE$$

Since N and $\Phi(E)$ are the same in both integrals and $E_{\text{threshold 1}}$ is approximately equal to $E_{\text{threshold 2}}$ for reasons explained later, the ratio $R1^{o}/R2^{o}$ is directly proportional to the energy integrated cross sections,

$$\frac{R1^{o}}{R2^{o}} = \int_{E_{threshold}}^{E_{maximum}} \sigma_1(E)dE \Big/ \int_{E_{threshold}}^{E_{maximum}} \sigma_2(E)dE$$

The ratio of $R1^{o}$ to $R2^{o}$ for both targets indicates that when the isomeric pair states in ^{91}Mo are populated by the ^{92}Mo(γ,n) reaction, the isomeric state is populated 1.97 (=414.9/211.1) times as frequently as the ground state. In the ^{94}Mo(γ,3n) reactions the isomeric state is produced 1.60(=12.25/7.67) times as frequently. The interpretation of these results will be discussed at length later.

IX. EXPERIMENTAL APPARATUS

A. Synchrotron, Irradiation Procedures, Transfer System

Irradiation of the isotopically separated target materials was performed in the same way as for the ^{192}Os targets used in the ^{190}Re work. In all cases the synchrotron internal probe position was used with the accelerator operating at its maximum energy. The samples were weighed into the small aluminum irradiation cans along with a previously weighed copper flux monitor foil which was positioned inside and toward the small end of the can. The can was then positioned with the probe so that the small end of the can would intercept the beam first.

For those systems with short lived products, the can was removed from the probe position after the irradiation and quickly transferred to the reactor building counting room using the transfer and timing system described in Part I.

B. Separated Isotope Targets, Copper Monitors

The isotopically separated target materials were obtained from the Stable Isotopes Division of the Oak Ridge National Laboratory, and were used without additional preparation. Table 8 lists the chemical and isotopic composition of these materials. The flux monitor foils were small disks of high purity copper metal approximately 3 mm in diameter and 1 mm thick. These foils were weighed prior to

Table 8. (Continued)

Element (Chemical form)	isotope	Isotopic analysis		
		Isotope	Atomic %	Precision
Nd (Nd$_2$O$_3$)	^{143}Nd	142	2.63	± 0.02
		143	91.32	0.05
		144	3.9	0.03
		145	0.77	0.02
		146	1.05	0.02
		148	0.23	0.02
		150	0.14	0.01
Nd (Nd$_2$O$_3$)	^{144}Nd	142	0.60	± 0.05
		143	0.57	0.05
		144	97.51	0.10
		145	0.68	0.05
		146	0.47	0.05
		148	0.10	0.02
		150	0.07	0.02

irradiation and washed with acetone and water before counting
to remove any surface contaminants.

C. Counting Equipment

In all cases the Ge(Li) detector and the 1600 channel
RIDL pulse height analyzer were used to count the activity
of the isomeric pair. Depending on the system studied and
the half-lives of the states, either full 1600 channel
spectra were accumulated or the analyzer memory was broken
up into 16 one hundred channel subgroups for spectrum
accumulation. This latter mode facilitated the measurement
of the decay curves for the short lived reaction products.

All of the targets were counted in plastic test tubes
positioned at the detector face. To correct for the Ge(Li)
detector's varying counting efficiency with energy, a number
of standard gamma-ray sources were counted at the detector
face. An efficiency curve similar to Figure 5 was constructed
from these data and used to make the efficiency corrections
like those illustrated in the sample calculations.

For three of the systems studied (^{91}Mo, ^{112}In, and
^{141}Nd) the half-lives of the nuclear states were relatively
short (1 min to 2.5 hr) (41,42,44). In these cases the 9.9
min ^{62}Cu activity of the monitor foils was used for the dose
measurements. A single channel analyzer with a scaler was
coupled to a 10.2 x 10.2 cm NaI(Tl) crystal for use in
counting the 511 keV gamma ray from the positron emitting

source. The copper foils were placed between two 25 cent

pieces to insure complete annihilation of the positrons. A

series of one minute counts after the irradiation were made

to construct the decay curve for the ^{62}Cu activity and to

measure the monitor activity at the end of the irradiation.

The ^{137}Ce system involved much longer lived states (9 and

34 hours) (43). For this case the 12.9 hour ^{64}Cu activity

of the monitor foils was used. Counting of the 1340 keV

^{64}Cu gamma ray was done with the 1600 channel analyzer and

the Ge(Li) detector.

D. Data Handling Procedures, Computer Programs

The spectral data from the 1600 channel analyzer were

punched onto paper tape. The same data handling procedures

as in the ^{190}Re work were used in transferring the paper

tape data onto magnetic tape or punched cards for computer

assisted data analysis. The spectrum analysis program

described in Part I (ICPEAX) was used for automatic photo-

peak searching and fitting in the spectra accumulated with

the Ge(Li) detector. A small computer program that

integrated the photopeak areas in time-sequenced spectrum

accumulations was used for the cases in which the analyzer

was set up to accumulate 16 one hundred channel spectra in

rapid succession. This program also plotted the decay

curves for the spectrum photopeaks which were then graphi-

cally analyzed for half-lives and activities.

One new computer program was developed in the course of this isomer ratio work. The Equations 4 through 7 which must be solved simultaneously for the $R1^o$ and $R2^o$ values are sufficiently complex to require considerable time spent in their solution by hand. A computer program (ISOMER) was developed to solve this system of equations on the IBM 360/65 computer at the Computation Center. The method used was essentially the same as that outlined in the sample calculations presented earlier.

Two versions of this program were written. Initially the program was written in FORTRAN IV for programs submitted in punched card form. The program was developed, and tested in this manner. However, the small amount of input and output for the program combined with a fairly large computer time requirement made the program an ideal one for use on the IBM 2741 computer terminals that are part of the IBM 360/65 Conversational Programming System. The program written in the C.P.S. PL/1 language was then used for essentially instantaneous processing of the data which was fed to the computer via keyboard terminals located at various places on the campus. Virtually all of the isomer ratio calculations were made in this way.

X. EXPERIMENTAL METHODS AND RESULTS

This section deals with the experimental methods and results obtained for the four systems studied. Each system required slightly different procedures due to the range of half-lives that were encountered in the various isomeric pair nuclear states, the chemical composition of the target materials, and the relative cross sections for the nuclear reactions of interest. Prior to the irradiation of the isotopically separated target materials, trial measurements were made using target materials of natural isotopic distribution and the same chemical composition as the isotopically separated targets. The success and reproducibility of these measurements confirmed the feasibility of the method which was then used with the isotopically separated targets. These results are discussed below.

A. The ^{91}Mo System

Radioactive sources of the ground and isomeric states in ^{91}Mo were prepared by synchrotron irradiation from targets consisting primarily of ^{92}Mo and ^{94}Mo. The greater yield of ^{91}Mo from the ^{92}Mo(γ,n) reaction relative to the ^{94}Mo(γ,3n) reaction suggested the use of smaller target weights of the ^{92}Mo material. Decreasing the ^{92}Mo target weight resulted in comparable count rates for the ^{91}Mo activities produced from the two targets. This resulted in smaller uncertainties

in the photopeak activities and measured half-lives since
the deadtime corrections performed by the analyzer would
then be approximately the same for both cases.

A typical gamma-ray spectrum of the ^{91}Mo activities is
shown in Figure 20. The 511 keV line is characteristic of
the decay of the positron emitting ground state of ^{91}Mo.
The γ-ray transition at 658 keV results from the decay of
the ^{91}Mo isomeric state to the ground state (41). The photo-
peak intensities were followed in time to construct decay
curves for both nuclear states. The half-lives determined
in this manner agreed with previously published measurements
(41). The isomer ratio calculations which were outlined in
Section VIII were performed using data from triplicate runs
on each of the two targets, utilizing the decay scheme
information of Cretzu, Hohmuth, and Schintlmeister (41).
The isomer ratio defined as the energy integrated cross
section for the production of the lower spin state (in this
case the 1/2$^-$, ^{91m}Mo activity) divided by the corresponding
quantity for the higher spin state (9/2$^+$, ^{91}Mo ground state)
was determined to be 1.92 $\pm$ 0.15 for the ^{92}Mo (γ,n) reaction
mode. The isomer ratio for the ^{94}Mo(γ,3n) reaction mode
was determined to be 1.59 $\pm$ 0.16. These isomer ratios are
the average of the three measurements. The uncertainties
are the average of the deviations of the three measurements
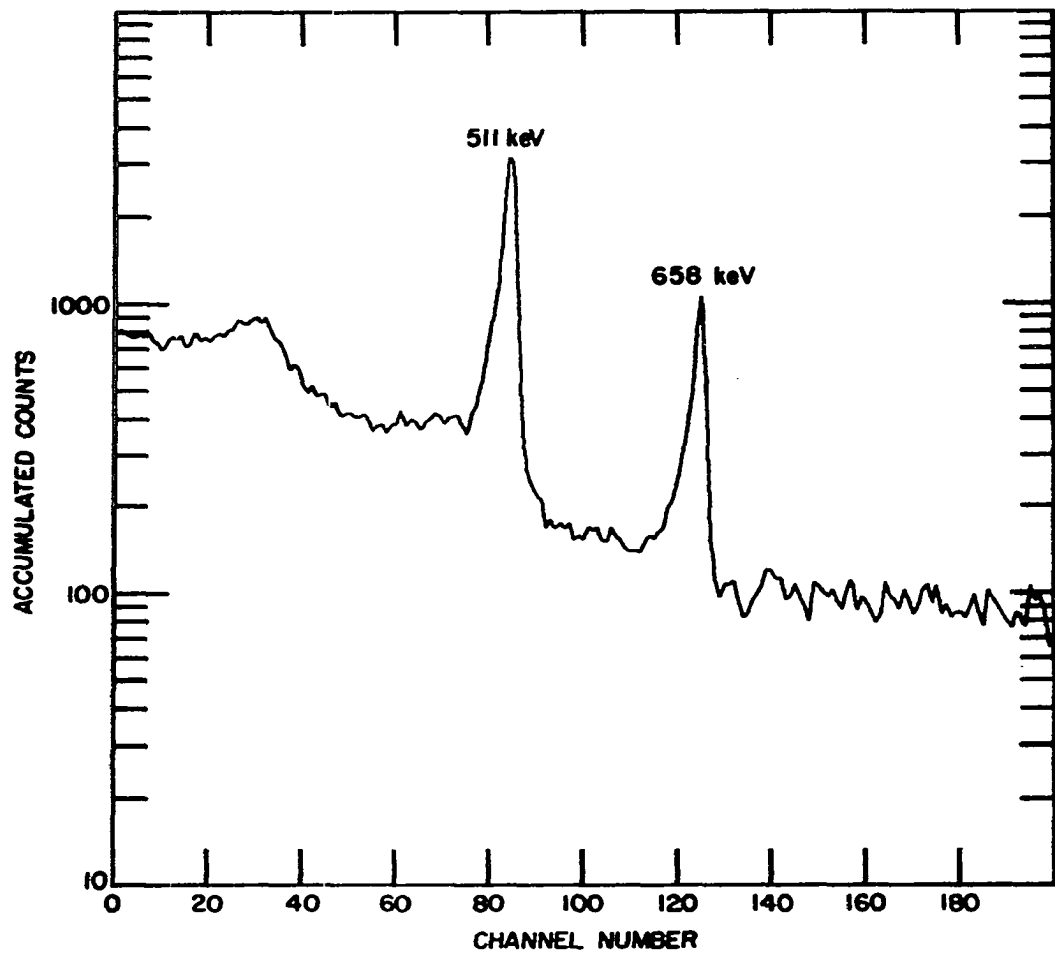for their average.

511 keV

658 keV

ACCUMULATED COUNTS

1000

100

10

0   20   40   60   80   100   120   140   160   180

CHANNEL NUMBER

Figure 20. Gamma-ray spectrum of the ^{91}Mo source

B. The ^{112}In System

The second system which was studied involved the pair

of isomeric states of ^{112}In. Targets of isotopically

separated ^{113}In$_2$O$_3$ and ^{115}In$_2$O$_3$ were irradiated in the

usual manner and counted with the Ge(Li) detector. A

typical γ-ray spectrum of the induced activities is shown

in Figure 21. The indium sources were generally allowed to

cool for a short period of time following the irradiation

so that the intense 511 keV annihilation radiation from the

decay of 2.1 min ^{15}O would not interfere with measurements

of the ^{112}In γ-ray transitions.

Decay curves for each of the isomeric states yielded

half-lives close to those published by Ruan and Yoshizawa in

their report on the decay of the ^{112}In activities (42).

Repeated attempts to calculate reproducible isomer ratios

for either reaction mode failed however. The isomer ratios

varied considerably when data accumulated at different times

after the irradiation were used. This behavior was observed

to a lesser extent when natural In$_2$O$_3$ targets were used and

the decay of the isomeric states was not followed as long.

The close agreement between the observed half-lives and

those previously reported discounted the possibility that

the decay corrections in Equations 4 through 7 caused this

problem. It was thought that two possible causes might be

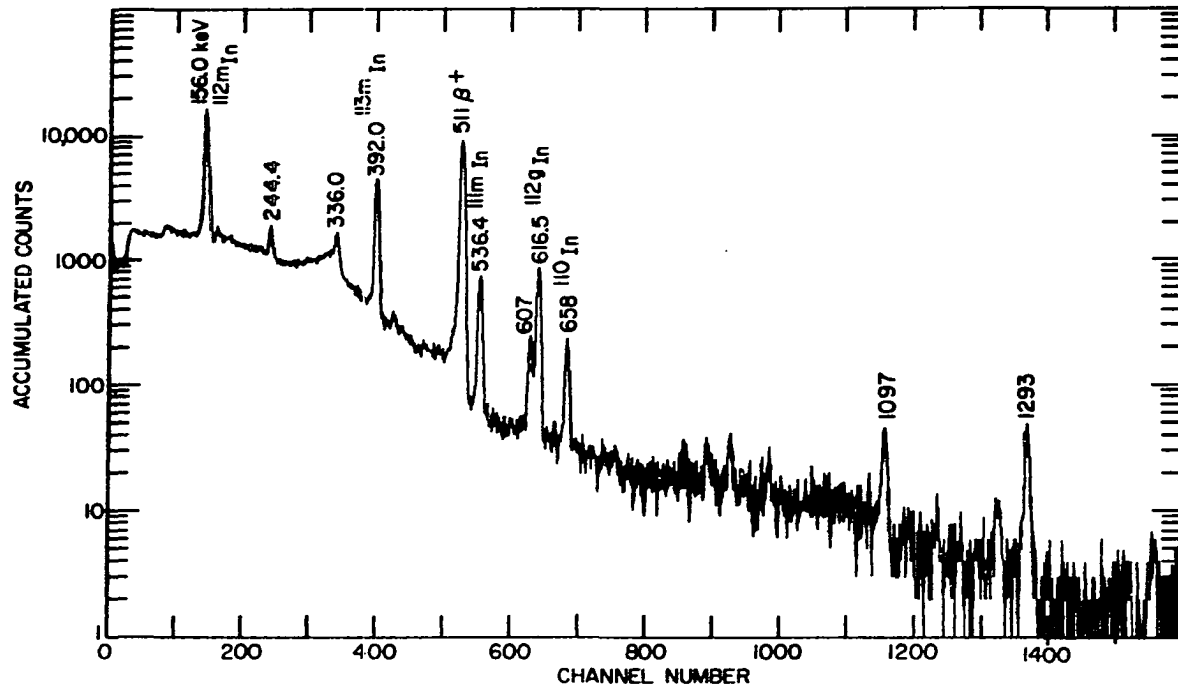an inaccurate value of the internal conversion coefficient

Figure 21. Gamma-ray spectrum of the ^{112}In source

for the isomeric transition in ^{112m}In or inaccurate measurement of the beta decay branching yield for the decay of the ^{112}In ground state. The conversion coefficient has been reported as 3.3 $\pm$ 0.7 for the K shell and 5.8 $\pm$ 1.2 for the K/L ratio and the branching yield as 6 percent (42). Trial calculations were made in which slight changes in these two parameters were included. Large variations in the calculated isomer ratio occurred when this procedure was tried. This indicated that without better measurements of one or both of these parameters the isomer ratios could not be reliably calculated except by an arbitrary adjustment of these parameters to yield reproducible results.

C. The ^{137}Ce System

A third system to be studied involved the production of the isomeric pair states in ^{137}Ce from targets of ^{138}Ce and ^{140}Ce. The isotopically separated targets were in the form of Ce_2O_3. The relatively long lived isomeric pair states (9 and 34 hours) allowed for a convenient cooling period after the irradiation so that the short lived radioactive products produced whenever oxygen is irradiated could decay before the target was counted. In Figure 22, a typical γ-ray spectrum of the activities induced in the cerium targets is shown. The 225 keV transition is characteristic of the decay of the ^{137m}Ce isomeric state, and the 446 keV transition of the ^{137}Ce ground state decay (43).

Figure 22. Gamma-ray spectrum of the 137Ce source
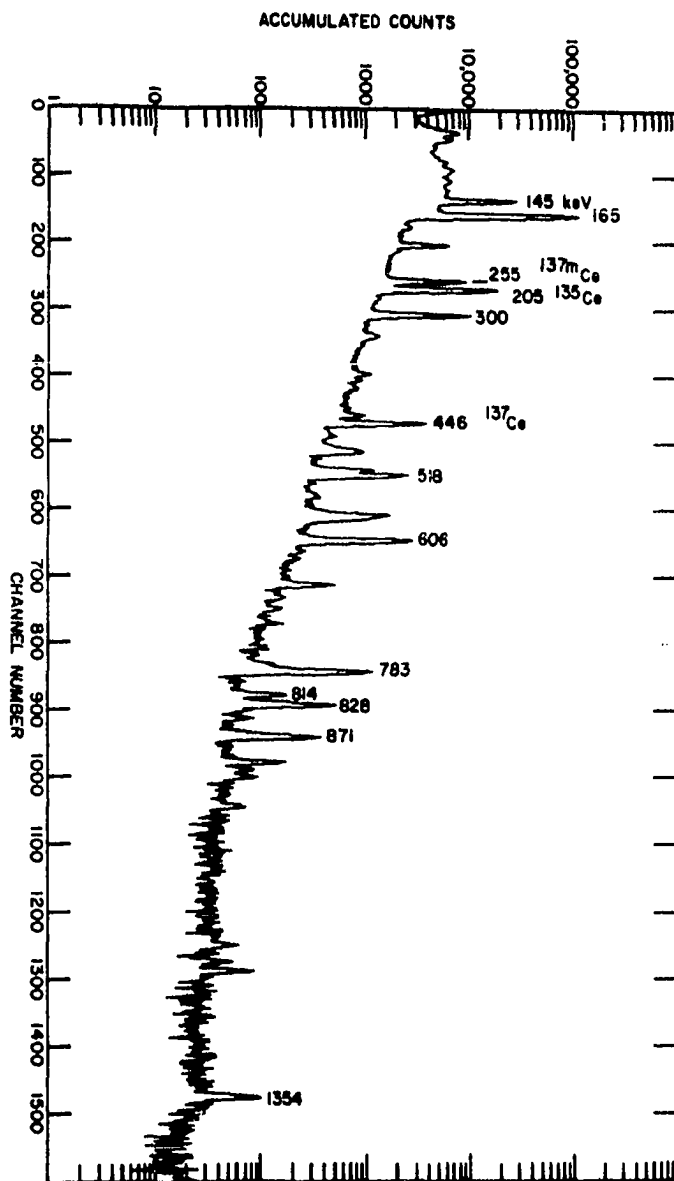
One modification to the data analysis procedure was required for the cerium system. The targets of $^{138}Ce_2O_3$ were available in an isotopic enrichment of only 14.32 percent in ^{138}Ce (compared with a natural abundance of 0.25 percent). These targets consequently contained large amounts of ^{140}Ce ($\sim$ 82 percent). Therefore the yield of ^{137}Ce from the enriched ^{138}Ce target was not solely due to the ^{138}Ce (γ,n) reaction, as was the case with reactions in the first two systems described above. The isomer ratio and relative cross sections for the $^{138}Ce(\gamma,n)$ reaction were however obtained by relating the measurements from both of the isotopically enriched targets to the measurements of the isomer ratio and reaction cross sections obtained using the natural cerium targets. In this manner, the following isomer ratios were obtained: 3.1 $\pm$ 0.1 for the $^{138}Ce(\gamma,n)$ ^{137}Ce reaction and 1.10 $\pm$ 0.12 for the $^{140}Ce(\gamma,3n)$ reaction. -

D. The ^{141}Nd System

Measurements of the (γ,n) and (γ,3n) isomer ratios for production of ^{141}Nd from ^{142}Nd and ^{144}Nd targets were complicated by the existence of the stable ^{143}Nd isotope. In the three previous systems no stable isotope existed between the two target nuclei. As can be seen in Table 9, small but significant amounts of ^{143}Nd were present in the isotopically enriched targets of ^{142}Nd and ^{144}Nd. To correct for the additional yield of ^{141}Nd from the $^{143}Nd(\gamma,2n)$ reactions,

targets enriched in $^{143}Nd_2O_3$ were irradiated in addition to the usual isotopically enriched targets of $^{142}Nd_2O_3$ and $^{144}Nd_2O_3$.

A typical γ-ray spectrum of the activities induced in the Nd targets is shown in Figure 23. Following the integration of photopeaks and construction of the decay curves for both activities of ^{141}Nd, the isomer ratios were determined in the usual manner. Corrections for the presence of ^{143}Nd in both targets were made. The resulting isomer ratios were 5.2 ± 0.3 for the $^{142}Nd(γ,n)^{141}Nd$ reaction and 1.8 ± 0.25 for the $^{144}Nd(γ,3n)$ reaction.

Figure 23. Gamma-ray spectrum of the ^{141}Nd source
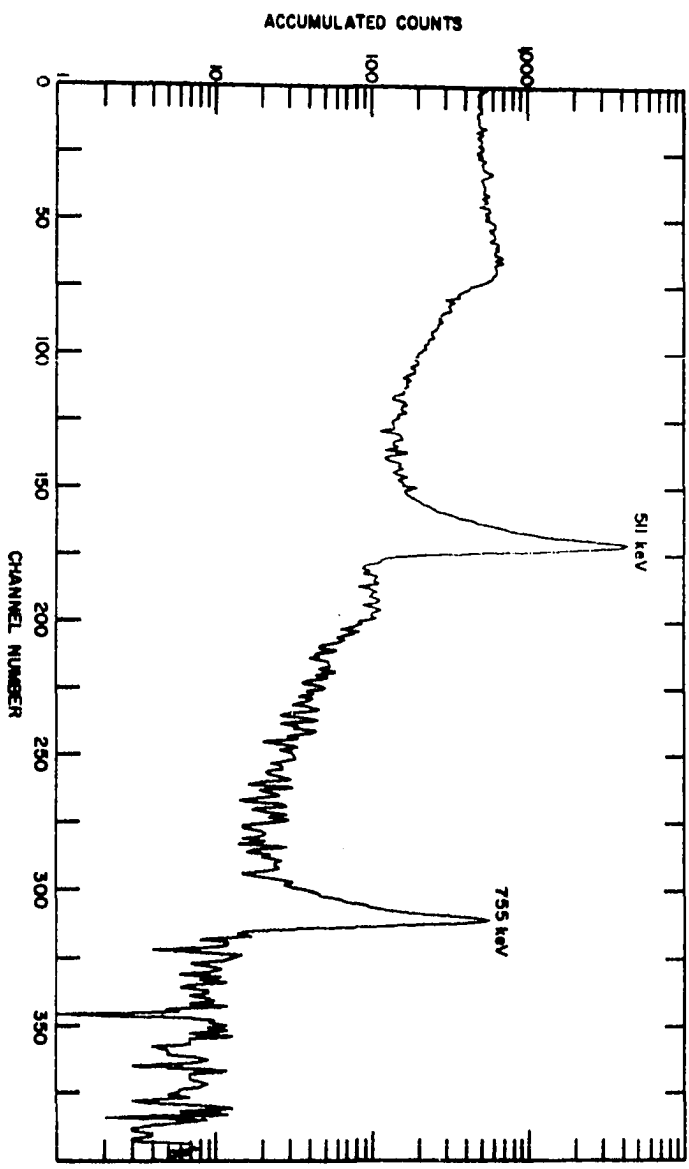
XI. DISCUSSION OF RESULTS AND THE TREATMENT OF ERRORS

A. Interpretation of the Experimental Results

A summary of the experimental results for the three systems in which reproducible isomer ratios could be calculated is shown in Table 9. The ratios are defined as the energy integrated cross section for the production of the lower spin state divided by the corresponding quantity for the higher spin state. Table 9 also contains the threshold energies for the production of the ground states by both reaction modes. The threshold energy for the production of the higher energy isomeric state differs from these quantities by an amount equal to the excitation energy of the isomeric state. This excitation energy is less than 0.8 MeV for all three of the systems. Hence the threshold energies which appear in Equation 9 are approximately equal. The slight differences in these quantities produce insignificant effects in the integral Equation 9 because the cross section ($\sigma_1(E)$ and $\sigma_2(E)$) are generally quite small immediately above the threshold energy which is the only portion of the integration region affected by setting the two threshold energies equal.

Within each system a general trend in the isomer ratio results was observed. For purposes of further discussion let the isomeric pair nucleus with atomic number Z and mass number A be denoted by the symbol ^{A}Z. The two radioactive

Table 9. Threshold energies and isomer ratios for the ^{91}Mo, ^{137}Ce, and ^{141}Nd systems

Reaction	Isomer ratio	Threshold[a]
^{92}Mo$(\gamma,n)^{91}$Mo	1.92 ± 0.15	13.13 MeV
^{94}Mo$(\gamma,3n)^{91}$Mo	1.59 ± 0.16	30.72
^{138}Ce$(\gamma,n)^{137}$Ce	3.1 ± 0.1	10.31
^{140}Ce$(\gamma,3n)^{137}$Ce	1.10 ± 0.12	26.34
^{142}Nd$(\gamma,n)^{141}$Nd	5.2 ± 0.3	9.79
^{144}Nd$(\gamma,3n)^{141}$Nd	1.80 ± 0.25	23.67

[a]Calculated using data from reference (26).

states in ^{A}Z were separately produced by the $^{A+1}$Z$(\gamma,n)^{A}$Z $^{A+3}$Z$(\gamma,3n)^{A}$Z reactions. The isomer ratios for the $^{A+1}$Z(γ,n) reactions in each of the three systems indicated that the state with lower spin (whether the ground state or the isomeric state) was produced to a greater extent than the higher spin state. This behavior has been frequently observed before and has been explained with the notion that the neutron emitting states of the compound even-even nucleus have spins of one, corresponding to the absorption of El photons by the target nucleus. The compound nucleus can then decay

more readily to the lower spin state in the product nucleus
by the emission of a low angular momentum neutron and low
multipolarity gamma rays rather than by higher (and conse-
quently more hindered) angular momentum processes leading
to the higher spin state. In the case of the $^{A+3}Z(\gamma,3n)^A Z$
isomer ratios however the two states in the product nucleus
were observed to be more equally populated (the isomer
ratios were closer to unity). The following material
attempts to explain this behavior.

One explanation involves the nature of the neutron
emitting states in the ^{A+3}Z target nucleus that are produced
by photonuclear excitation. It has been pointed out that
absorption of higher energy gamma rays by a nucleus generally
results in the population of higher angular momentum states
in the compound nucleus (36). As has been previously
discussed, the $^{A+1}Z(\gamma,n)^A Z$ reactions on even-even targets
usually proceed through the population of spin one neutron
emitting states of the compound nucleus. This situation is
not quite the same in the $^{A+3}Z(\gamma,3n)^A Z$ reactions. In this
situation the higher reaction threshold energy naturally
results in the population of higher energy photoabsorption
states in the compound nucleus. These states will on the
average have higher spins than the corresponding photo-
absorption states in the $^{A+1}Z(\gamma,n)^A Z$ reactions. It should
also be noted that lower energy absorption states in the

^{A+3}Z nucleus will also be populated and result in side reactions of the type $^{A+3}Z(\gamma,n)^{A+2}Z$ or $^{A+3}Z(\gamma,2n)^{A+1}$, yielding other stable or radioactive products. Following the production of these higher spin states in the ^{A+3}Z compound nucleus, neutron emission will occur which will ultimately yield the two radioactive states in the ^{A}Z product nucleus. This triple neutron emission from the ^{A+3}Z compound nucleus will consequently start from a higher spin state than the single neutron emission from the ^{A+1}Z compound nucleus. This situation favors the production of the higher spin isomeric state in the ^{A}Z product nucleus which in turn causes the isomer ratio to become closer to one.

A second explanation for the behavior of the isomer ratios concerns the spread of final angular momentum states that can be reached by the triple neutron emission process over that of a single neutron emission. If one assumes that only $l = 0$ (s-wave) neutrons are emitted from the ^{A+1}Z and ^{A+3}Z compound nuclei, then the range of spins of the final states reached in the decay of the ^{A+3}Z compound nucleus will be larger than those in the ^{A+1}Z decay. This is the result of the many additional angular momentum states that can be reached by coupling the three $s = 1/2$ neutrons spins to the spin of the ^{A+3}Z absorption states. Subsequent gamma-ray emission can then populate additional states leading to a

more equal yield of the two isomeric states in the $^{A+3}Z(\gamma,3n)$ reaction mode. Allowing $1 > 0$ neutron emission again causes a greater spread in the available final angular momentum states, producing a larger yield of the higher spin state.

Both of these explanations may be invoked to explain the experimental results. In all likelihood both processes do occur and are reflected in the trend that has been observed in the systems so far studied.

B. Discussion of Errors

The following section deals with an analysis of the errors inherent in the measurements of the isomer ratios. Random errors and their effects are first treated, followed by a similar treatment for systematic errors.

The three major sources of error that might randomly affect the isomer ratio measurements involve the fluctuations of bean intensity during the irradiation, the positioning of the targets relative to the beam path, and the positioning of the targets for counting. The radioactive kinetics equations which describe the production reaction and decay processes are valid only in the case of a nonfluctuating beam intensity striking the targets. Fluctuations of the beam intensity with time cause nonuniform production of the product nuclei, especially when the period of the beam fluctuations is approximately the same as the half-lives of the radioactive products. This problem can be minimized by

keeping the irradiation duration short compared to the half-lives of the product nuclei whenever possible.

The second problem concerns the positioning of the targets in the beam so that reproducible irradiation geometry is achieved for different targets in which cross section measurements for the two different reaction modes are related. The comparable dose measurements obtained from the copper monitor foils indicated that this target positioning problem can easily be minimized by careful adjustment of the irradiation geometry using the probe fastening device which prevents movement of the probe during the irradiation.

The third source of random errors arises from non-reproducible positioning of the target materials for counting. Due to the low yields of the product activities, counting at the detector face was required. Hence, slight differences in counting geometry between targets would tend to introduce errors in quantities derived from measurements of the activities in two difference targets. Again careful attention to sample positioning prior to counting minimizes this source of random error.

Systematic errors affecting the isomer ratio measurements will have varying degrees of importance. Relatively minor effects will be caused by systematic errors involved with the weighing of the target materials and monitor foils.

Inaccurate measurements of the isotopic composition of the mass separated target materials will also cause slight systematic errors in the isomer ratio results. Similarly inaccurate timing measurements of the irradiation duration and counting intervals will introduce slight systematic errors. However these three effects are relatively minor sources of systematic error when compared to those errors introduced by inaccurate decay scheme information.

Calculation of the isomer ratios relies heavily on previously published decay scheme information for the activities produced during the irradiation. In particular the measurements of gamma-ray internal conversion coefficients and beta decay branching percentages strongly affect the calculated isomer ratios. Substantial systematic errors are most likely in these cases since these two quantities are used as correction factors to obtain the absolute yields of the isomeric pair activities.

Estimates of the combined effects of these random and systematic errors are difficult to make. It was thought that the best way to report these isomer ratio measurements was in the manner described in Section X of this part of the thesis, with the understanding that the major source of possible systematic error arises from inaccurate decay scheme information as discussed above.

XII. FUTURE WORK

The foregoing material represents an initial attempt to measure and interpret several isomer ratios for nuclides produced by two different reaction pathways. The four cases which were studied were chosen largely because of the convenient experimental methods which could be used in each system. The combination of readily available isotopically separated target materials, well characterized decay schemes, and convenient half-lives suggested the four systems which were studied. Several additional systems could be investigated. These unfortunately would be somewhat less favorable situations involving very short or very long lived nuclear states with less readily detectable characteristic radiations, more poorly studied decay schemes, with production reactions requiring more expensive separated targets. The situation is by no means hopeless but more effort would be needed to apply the method described in this thesis to additional systems.

A number of other investigations suggest themselves. Future work aimed at reducing the uncertainties and errors of measurement described in Section XI is one such possibility. Another would be to measure the isomer ratios as a function of beam energy to perhaps correlate the cross section measurements with particular photon absorption energies rather than measuring the composite isomer ratios

resulting from a number of absorption processes induced by the broad bremsstrahlung spectrum.

XIII. LITERATURE CITED

1. Becquerel, H., Compt, rend., $\underline{122}$, 432 (1896).

2. Joliot, F. and Curie, I., Nature, $\underline{133}$, 201 (1934).

3. Fermi, E., Z. Physik, $\underline{88}$, 161 (1934).

4. Haxel, O., Jensen, J. H. D. and Suess, H. E., Z. Physik, $\underline{128}$, 295 (1950).

5. Mayer, M. G., Phys.Rev., $\underline{78}$, 16 (1950).

6. Aten, A. H. W., Jr. and de Feyfer, G. D., Physica, $\underline{21}$, 543 (1955).

7. Baro, G. B. and Flegenheimer, J., Radiochim. Acta, $\underline{1}$, 2 (1962).

8. Kane, W. R., Emery, G. T., Scharff-Goldhaber, G. and McKeown, M., Phys. Rev., $\underline{119}$, 1953 (1960).

9. Mariscotti, M. A., Kane, W. R. and Emery, G. T., AEC Report BNL-11426, Brookhaven National Lab., Upton, N.Y., 1967.

10. Castern, R. F. X., "Collective nuclear structure studies in the osmium nuclei," unpublished Ph.D. thesis, New Haven, Conn., Library, Yale University, 1967.

11. Hammer, C. L. and Bureau, A. J., Rev. Sci. Instrum., $\underline{26}$, 594 (1955).

12. Hammer, C. L. and Bureau, A. J., Rev. Sci. Instrum., $\underline{26}$, 598 (1955).

13. Bureau, A. and Hammer, C., Rev. Sci. Instrum., $\underline{32}$, 93 (1961).

14. Korthoven, P. J. M. and Carlsen, F. S., AEC Report IS-1501, Ames Lab., Ames, Iowa, 1966.

15. Scharff-Goldhaber, G., Alburger, D. E., Harbottle, G. and McKeown, M., Phys. Rev., $\underline{111}$, 913 (1958).

16. Nablo, S. V., Johns, M. W. and Goodman, R. H., Can. J. Phys., $\underline{36}$, 1409 (1958).

17. Lederer, C. M., Hollander, J. M. and Perlman, I., "Table of Isotopes," 6th ed., J. Wiley and Co., New York, N.Y., 1967, p 561.

18. Aten A. H. W., Jr. and de Feyfer, G. D., Physica, 19, 1143 (1953).

19. Smith, J., "OPLSPA, a computer program for least-squares fitting," unpublished computer program description, Ames, Iowa, Computation Center Library, Iowa State University of Science and Technology, 1964.

20. Korthoven, P. J. M., AEC Report IS-1811, Ames, Lab., Ames, Iowa, 1967.

21. Yamazaki, T., Ikegami, H. and Sakai, M., Nucl. Phys., A, 131, 169 (1969).

22. Harmatz, B. and Handeley, T. H., Nucl. Phys., 56, 1 (1964).

23. Bearden, J. A. and Burr, A. F., AEC Report NYO-2543-1, New York Operations Office, AEC, 1965.

24. "Beta and Gamma-Ray Spectroscopy," Siegbahn, K. editor, North-Holland Publishing Co., Amsterdam, 1955, p 273.

25. Nichols, R. T., McAdams, R. E. and Jensen, E. N., Phys. Rev., 122, 172 (1961).

26. Hillman, M., AEC Report BNL-846(T-333), Brookhaven National Lab., Upton, N.Y., 1964.

27. Friedlander, G., Kennedy, J. W. and Miller, J. M., "Nuclear and Radiochemistry," 2nd ed., J. Wiley and Co., New York, N.Y., 1967, p 245.

28. Lindstrom, B. and Marklund, I., Nucl. Phys., 49, 609 (1963).

29. Davydov, A. S. and Filippov, G. F., Nucl. Phys., 8, 237 (1958).

30. Davydov, A. S. and Chaban, A. A., Nucl. Phys., 20, 499 (1960).

31. Davidson, J. P., Nucl. Phys., 33, 664 (1962).

32. Kumar, K. and Baranger, M., Nucl. Phys., A, <u>122</u>, 273 (1968).

33. Kumar, K., Phys. Lett., <u>29B</u>, 1 (1969).

34. Abecasis, S. M. and Bosch, H. E., Nuovo Cimento, A, <u>53B</u>(10), 147 (1968).

35. Segre, E., Halford, R. S. and Seaborg, G. T., Phys. Rev. <u>55</u>, 321 (1939).

36. Huizenga, J. R. and Vandenbosch, R., Phys. Rev., <u>120</u>, 1305 (1960).

37. Levinger, J. S., "Nuclear Photodisintegration," Oxford University Press, Oxford, England, 1960.

38. Wing, J., AEC Report ANL-6598, Argonne National Lab., Lemont, Ill., 1962.

39. "Photonuclear Reactions," Bibliographical series No. 10, International Atomic Energy Agency, Vienna, Austria, 1964.

40. "Photonuclear Reactions," Vol. II (1963-1966), Bibliographical series No. 27, International Atomic Energy Agency, Vienna, Austria, 1967.

41. Cretzu, V. T., Hohmuth, K. and Schintlmeister, J., Ann. Physik, <u>16</u>, 312 (1965).

42. Ruan, J. Z. and Yoshizawa, Y., J. Phys. Soc. Jap., <u>17</u>, 6 (1962).

43. Frankel, R. B., Shirley, D. A. and Stone, N. J., Phys. Rev., B, <u>136</u>, 577 (1964).

44. Kochler, D. R. and Grissom, J. T., Nucl. Phys., <u>84</u>, 235 (1966).

45. Costa, S., Ferrero, F., Ferroni, S., Pasqualini, L. and Silva, E., Nucl. Phys., <u>72</u>, 158 (1965).

46. Friedlander, G., Kennedy, J. W. and Miller, J. M., "Nuclear and Radiochemistry," 2nd ed., J. Wiley and Co., New York, N.Y., 1967, pp 78-81.

XIV. ACKNOWLEDGMENTS